

Adaptive Formal Approximations of Markov Chains

Alessandro Abate^a, Roman Andriushchenko^b, Milan Češka^{b,*}, Marta Kwiatkowska^a

^a*Department of Computer Science, University of Oxford, Oxford, UK*

^b*Faculty of Information Technology, Brno University of Technology, Brno, Czech Republic*

Abstract

We explore formal approximation techniques for Markov chains based on state-space reduction that aim at improving the scalability of the analysis, while providing formal bounds on the approximation error. We first present a comprehensive survey of existing state-reduction techniques based on clustering or truncation. Then, we extend existing frameworks for aggregation-based analysis of Markov chains by allowing them to handle chains with an arbitrary structure of the underlying state space – including continuous-time models – and improve upon existing bounds on the approximation error. Finally, we introduce a new hybrid scheme that utilises both aggregation and truncation of the state space and provides the best available approach for approximating continuous-time models. We conclude with a broad and detailed comparative evaluation of existing and new approximation techniques and investigate how different methods handle various Markov models. The results also show that the introduced hybrid scheme significantly outperforms existing approaches and provides a speedup of the analysis up to a factor of 30 with the corresponding approximation error bounded within 0.1%.

Keywords: Markov models, probabilistic model checking, approximation techniques, adaptive aggregation

1. Introduction

Probability plays a prominent role in the design and modelling of systems with unpredictable or unreliable behaviour. Markov chains are a class of such probabilistic models that have been extensively used in many areas of Science
5 and Engineering, including the analysis of performance of computer networks and of reliability of communication and security protocols [1, 2], in the study of various quantitative attributes of biochemical reaction networks [3, 4] or genetics [5]. A Markov chain can be thought of as a collection of states accompanied
10 by a function that describes the probabilistic nature of transitions between any pair of states. Depending on the type of model, these transitions can occur

*Corresponding author

in discrete or continuous time. The study of such chains is carried out either analytically, or through exhaustive exploration of its execution paths, or by employing numerical schemes (usually by solving a system of equations providing precise or approximate solutions of the chains). For the analysis of continuous-
15 time models, a typical method employed is uniformisation, which is based on a time-discretisation of the chain of interest [6]. Prominent tools allowing to analyse and verify Markov models include PRISM [7], STORM [8], or MODEST [9].

Unfortunately, efficient analysis of Markov models is difficult to achieve in practice due to the state explosion problem. In order to enable the handling
20 of larger state spaces, several model approximation techniques have been introduced. These techniques typically solve a smaller chain – one with a reduced state space – and then interpret results in terms of the original model. State-aggregation methods [10] construct this smaller chain by clustering (or lumping, namely aggregating) the state space. State-space truncation methods [6], on the
25 other hand, work by dynamically neglecting states with insignificant transient probability (later we will define transient probability as the probability mass at any given time). In both cases an approximation error must be quantified. In practice, highly accurate probability approximations are crucial, for example in reliability analysis of safety-critical systems or when checking satisfiability of
30 temporal logic formulae.

1.1. Key contributions

In this work, we present a comprehensive survey of existing state-reduction techniques for Markov chains and focus on the enhancement of a framework [10] (by the same authors) for aggregation-based analysis. In particular, the new
35 improvements presented in this article include:

- the design of more accurate bounds on the approximation error (Subsections 3.1-3.2)
- the development of an accurate and efficient clustering (aggregating) method applicable to chains with an arbitrary structure of the underlying state
40 space (Subsections 3.4-3.5)
- the integration of aggregation with uniformisation (i.e. time discretisation) to enable the analysis of continuous-time models (Subsections 4.1-4.2)
- the design of a new hybrid scheme that utilises both aggregation and truncation of the state space and provides the best available approach for
45 approximating continuous-time models (Subsection 4.3)
- the first in-depth performance evaluation of all available reduction techniques on a broad range of case studies (Section 5)

In order to perform a fair experimental evaluation of the presented approximation techniques, a total of eight methods for Markov chain analysis (5 existing
50 and 3 new ones) are implemented in the probabilistic model checker PRISM [7]. First, we showcase the developed framework for the aggregation-based analysis,

highlight its improvement in both precision and speedup as compared to [10], and confirm that the resulting aggregating method can provide a valid model approximation along with precise error bounds, both in discrete and continuous
55 time. Further, we perform the first in-depth performance evaluation of all available reduction techniques using a broad range of case studies and investigate how different methods handle various classes of models. Finally, we demonstrate that a new hybrid method significantly outperforms existing approaches and provides speedup of the analysis up to a factor of 30 with the corresponding
60 approximation error bounded within 0.1%.

1.2. Related work

Lumping (i.e. state-space aggregation) is a widely studied approach to achieve state-space reduction allowing to analyze large Markov Chains. Theoretical concepts underlying lumpability have been first introduced in [11] and further developed e.g. in [12, 13] including extensions towards approximate notions such as
65 quasi-lumpable [14] or nearly completely decomposable [15, 16] Markov chains combined with a stochastic comparison approach [17]. The proposed algorithms usually focus on approximating steady-state distribution of discrete-time chains. Extensions towards the transient analysis and continuous-time are only discussed on a theoretical level. Another way to exploit a specific structure of
70 the chain is to use clustering based on (bi-)simulation equivalence [18], which uses symmetries of the concrete model and performs exact numerical computation. The common limitation of the aforementioned methods is that they can be applied only to specific Markov chains.

To enable handling of models with a more general structure, advanced notions of approximate equivalence have been introduced [19], which have led to new abstraction techniques for the numerical analysis of labelled Markov chains with finite [20] as well as with uncountably infinite state spaces [21, 22]. The work in [23] presents an algorithm to approximate probability distributions of a
80 Markov model forward in time, which inspired the adaptive scheme we proposed in [10] and further extended in this paper, where a formal error analysis steers the adaptation. This use of derived error bounds allows far greater accuracy and flexibility of the aggregation, as it accounts also for the history of the transient probability within specific clusters.

85 Stochastic biochemical systems, in particular, have given rise to a number of specialised methods for approximate analysis. Such systems are described using the language of Chemical Reaction Networks (CRNs). The time-evolution of CRNs is governed by the Chemical Master Equation (CME) [24] leading in general to infinite-state continuous-time Markov chains. To enable the analysis
90 of networks exhibiting complex dynamics, various approximation techniques have been proposed. These include, for example, the Linear Noise Approximation [20], where a Gaussian process approximates a CME and describes the time evolution of expectation and variance of the species in terms of a set of ordinary differential equations (ODEs). Recently, an aggregation scheme over ODEs that
95 aims at understanding the dynamics of large CRNs has been proposed in [25]. These deterministic approximations, however, cannot adequately capture the

stochasticity of CRNs caused by low population species. In order to cope with such systems, various hybrid models have been proposed [26, 27], where the dynamics of low population species are encompassed by a discrete stochastic process and the dynamics of large population species is approximated by a continuous one. These methods, however, do not provide any formal guarantees on the approximation error. In [28], a novel semi-quantitative framework for the analysis of CRNs has been introduced. It leverages population-based abstraction and introduces accelerated transitions to adequately capture a chain of the concrete transitions required to change the population level. The framework offers greater performance and scalability compared to existing techniques, although a formal guarantee is missing.

An alternative numerical method to deal with large or even infinite state spaces is truncation, which works by dynamically neglecting insignificant states with a transient probability below a given threshold. This method provides under-approximation of the true probability distribution, where the probability loss serves as an error bound. In the context of continuous-time chains, a combination of truncation with adaptive uniformisation [29] is a widely used technique known as fast adaptive uniformisation (FAU) [6], where the adaptivity allows to dynamically change the uniformisation rate: this significantly decreases the number of performed uniformisations on the chain. A reduction of the state space is achieved since usually a significant percentage of the transient probability is concentrated in a small subset of states and a large fraction of the state space can be thus truncated. However, when transient probability is spread over a large number of states, these methods can result in small reduction – or poor precision if a larger probability threshold is used.

Simulation-based methods qualitatively analyse the behaviour of a Markov chain by generating its trajectories: collecting the statistics from multiple realisations then allows to estimate the transient probability distribution. Simulation-based techniques include e.g. Gillespie’s Stochastic Simulation Algorithm [30] as well as its various modifications [31, 32, 33, 34]. These methods do not provide formal bounds on the error and instead can give weak precision guarantees in the form of confidence intervals. Furthermore, a large number of simulations is required to provide precise results, which can be very time consuming. Nonetheless, these practical approaches are suitable for situations where highly accurate estimates of the transient probability distribution are not necessary.

1.3. Structure of the article

In Section 2 we present an overview of existing approximate techniques for the analysis of Markov chains, namely, state-space aggregation and truncation, and review the uniformisation technique, including its fast adaptive version. In Section 3 we redefine notion of a state-space aggregation of a discrete-time Markov chain, introduce algorithms that allow us to approximate chains with arbitrary structure of the state space, explore various aggregation strategies and design a more precise approximation error bound. Then, in Section 4, we combine these results with uniformisation techniques to enable the handling of continuous-time models and introduce a new hybrid scheme that utilises both

aggregation and truncation of the state space. Finally, in Section 5 we discuss experimental results.

2. Preliminaries

145 In this section, we review the necessary theory and introduce notation that will be used throughout the paper. First, we discuss discrete-time Markov chains, describe state-space truncation and summarise aggregation approach presented in [10]. Then we consider continuous-time models and describe the uniformisation technique used for their analysis.

2.1. Discrete-time Markov chains

150 **Definition 1.** A (time-homogeneous) discrete-time Markov chain (DTMC) is a pair $D = (S, P)$, where

- S is the state space, and
- $P: S \times S \rightarrow [0, 1], \forall r \in S: \sum_{s \in S} P(r, s) = 1$, is the transition probability matrix.

155 Unless stated otherwise, we assume that the state space S is finite. The model is initialised via the probability distribution $\mathbf{p}_0: S \rightarrow [0, 1], \sum_{s \in S} \mathbf{p}_0(s) = 1$, and its transient probability distribution at time step $k > 0$ is

$$\mathbf{p}_k(s) = \sum_{r \in S} \mathbf{p}_{k-1}(r) \cdot P(r, s), \quad (1)$$

160 or, using matrix notation, $\mathbf{p}_k = \mathbf{p}_{k-1} \cdot P$. The act of performing one such multiplication is called an *iteration*, a *probability propagation*, or a *discrete-time step*. The problem of finding transient probability distribution \mathbf{p}_k at an arbitrary time horizon $k \geq 0$ is referred to as *the transient analysis* of the chain. Transient analysis is a key procedure for the quantitative verification of Markov chains against time-bounded specifications [7], where highly accurate approximations of probability distributions are crucial. Computing transient probability distributions directly using (1) suffers from the state-space explosion problem, and we are therefore interested in providing efficient and accurate approximations.

2.2. State-space aggregation of DTMC

170 In this subsection, we briefly describe the state-space aggregation method, as it was presented in [10], from where we adopt the corresponding notation¹. We omit some technical details and discuss them later in Section 3, where the generalised framework for state-space aggregation is developed.

¹An alternative approach to construct aggregated chains and, in particular, aggregated matrices, is via so-called *distributor* and *collector* matrices, as presented in [12]. In this paper, we focus on more general aggregations that are not always expressible using this related notation.

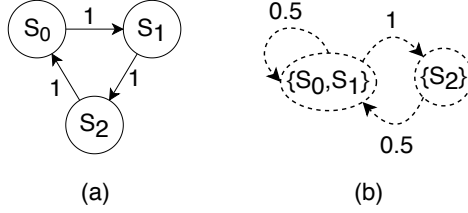


Figure 1: In (a) we consider a simple DTMC with three states; in (b) we construct its aggregation based on the partition $\Phi = \{\{s_0, s_1\}, \{s_2\}\}$, where the abstract transition matrix Π is computed using (19) – notice that in this case Π is not stochastic.

175 Let $D = (S, P)$ be a DTMC initialised via the probability distribution \mathbf{p}_0 ,
and assume that we are interested in approximating its transient probability
distribution \mathbf{p}_k , $k > 0$. Let Φ be a partition (clustering, aggregation) of the
state space S . We treat clusters in Φ as abstract states of a new aggregated
chain $\Delta = (\Phi, \Pi)$, where Π represents a suitable abstract transition probability
180 matrix $\Pi: \Phi \times \Phi \rightarrow \mathbb{R}_{\geq 0}$, as Figure 1 illustrates. Note that we do not require the
normalisation condition $\forall \rho \in \Phi: \sum_{\sigma \in \Phi} \Pi(\rho, \sigma) = 1$ to hold: in other words, the
obtained Π might not be a stochastic matrix and the abstract chain Δ might
not necessarily be a DTMC, as per Definition 1: implications of this choice are
discussed later. Abstract chain Δ is initialised using the (abstract) probability
185 distribution $\boldsymbol{\pi}_0: \Phi \rightarrow \mathbb{R}_{\geq 0}$, computed as

$$\boldsymbol{\pi}_0(\sigma) = \sum_{s \in \sigma} \mathbf{p}_0(s), \quad (2)$$

i.e. the probability of residing in cluster σ is the sum of transient probabilities
for the concrete states in σ . We can now recursively compute abstract transient
probability distribution $\boldsymbol{\pi}_k$ of Δ using vector-matrix multiplications, similar
190 to (1), as:

$$\boldsymbol{\pi}_k = \boldsymbol{\pi}_{k-1} \cdot \Pi. \quad (3)$$

Having obtained $\boldsymbol{\pi}_k$, i.e. the abstract probabilities of residing in individual clusters
at time k , the approximation $\tilde{\mathbf{p}}_k: S \rightarrow \mathbb{R}_{\geq 0}$ of the transient probability
distribution \mathbf{p}_k is defined as

$$\tilde{\mathbf{p}}_k(s) = \frac{\boldsymbol{\pi}_k(\sigma)}{\llbracket \sigma \rrbracket}, \quad s \in \sigma, \quad (4)$$

195 where $\llbracket \sigma \rrbracket$ denotes the cardinality of the set σ (namely the number of concrete
states comprising cluster σ). The intuition behind Equation (4) is that by
clustering several states into one abstract state σ , we no longer differentiate
between individual states, and therefore the probability of residing in cluster σ
200 is distributed uniformly among its concrete states.

If we select a partition Φ such that $\llbracket \Phi \rrbracket \ll \llbracket S \rrbracket$, working with the abstract chain (Φ, Π) and performing vector-matrix multiplications (3) allows to approximate \mathbf{p}_k using $\boldsymbol{\pi}_k$, and to reduce the computational demands when compared to performing the discrete steps in (1) with the concrete model. Let $\mathbf{e}_k := \tilde{\mathbf{p}}_k - \mathbf{p}_k$ denote an error vector associated with this approximation. We cannot compute this vector directly since we do not know the exact probabilities \mathbf{p}_k . However, we can formally bound the L_1 -norm $\|\mathbf{e}_k\|_1$ of this vector. This norm is efficiently computable from the structure of (Φ, Π) and can be used in the point-wise estimate of the transient probability. Namely, since $|\mathbf{e}_k(s)| \leq \|\mathbf{e}_k\|_1$, then it holds that $\mathbf{p}_k(s) = \tilde{\mathbf{p}}_k(s) \pm \|\mathbf{e}_k\|_1$. In order to estimate $\|\mathbf{e}_k\|_1$, introduce the quantity

$$\epsilon(\rho, \sigma) := \max_{s \in \sigma} \left| \Pi(\rho, \sigma) - \frac{\llbracket \sigma \rrbracket}{\llbracket \rho \rrbracket} \sum_{r \in \rho} P(r, s) \right| \quad (5)$$

and further denote $\epsilon(\rho) := \sum_{\sigma \in \Phi} \epsilon(\rho, \sigma)$. Then for the L_1 -norm of the error vector at time $k > 0$ it holds that

$$\|\mathbf{e}_k\|_1 \leq \|\mathbf{e}_{k-1}\|_1 + \sum_{\rho \in \Phi} \boldsymbol{\pi}_{k-1}(\rho) \cdot \epsilon(\rho), \quad (6)$$

where

$$\|\mathbf{e}_0\|_1 = \sum_{s \in S} |\mathbf{p}_0(s) - \tilde{\mathbf{p}}_0(s)|. \quad (7)$$

The term $\|\mathbf{e}_0\|_1$ is called *aggregation error* and describes the inaccuracy introduced when the exact \mathbf{p}_0 is replaced with $\tilde{\mathbf{p}}_0$. Additionally, during each discrete step, a *propagation error*, associated with the use of the abstraction Π instead of P , is produced and is captured by $\epsilon(\cdot, \cdot)$: this quantity accounts for the maximum difference, for a given pair of clusters, between the abstract transition probability and (rescaled) incoming probability. The product $\boldsymbol{\pi}_{k-1}(\rho) \cdot \epsilon(\rho)$ provides an upper bound on the error generated from ρ ; the sum over all abstract states in (6) then yields the overall error. The reason for computing the bound on the L_1 -norm of \mathbf{e}_k (and not \mathbf{e}_k itself) is that, as was already mentioned, we want to reduce the computational complexity of the error estimation: Equation (6) suggests that each step of this estimation is equivalent to performing a scalar product of two vectors in the aggregated setting (i.e. the one with the reduced state space).

So far, we have ignored how the partition Φ of S and how the abstract transition probability matrix Π are computed. In [10], where this approach is used to analyse biochemical processes, the aggregation is constructed based on the known structure of the model and on the underlying physics. Later, in Section 3, we will develop a generalized approach and describe how to aggregate chains with an arbitrary structure of their state space – until then, assume that a specific clustering is given. Eventually we will see that, as we perform discrete steps in the abstract setting, the probability distribution shifts, so adapting

the clustering of the state space can reduce the error: *an adaptive state-space aggregation* is therefore a method of using different clusterings sequentially in time, where the quality of each clustering is quantified by (6). In particular, assume that during transient analysis with a time horizon K we use L different clusterings, where the clustering $l \in \{1, \dots, L\}$ is used for k_l steps, $\sum_{l=1}^L k_l = K$, and the corresponding vector of error factors is ϵ^l . Similarly, let $\tilde{\mathbf{p}}_k^l, \boldsymbol{\pi}_k^l$ or \mathbf{e}_k^l denote the corresponding quantity during k -th step of the l -th clustering. Let $\mathbf{p}_0^1 = \mathbf{p}_0$ denote the initial probability distribution and let $\mathbf{p}_0^{l+1} = \tilde{\mathbf{p}}_{k_l}^l$ denote the initial (approximate) probability distribution used before $(l+1)$ -th clustering. The overall approximation error is the sum of errors obtained during each clustering:

$$\|\mathbf{e}_K\|_1 = \sum_{l=1}^L \|\mathbf{e}_{k_l}\|_1 \leq \underbrace{\sum_{l=1}^L \|\mathbf{p}_0^l - \tilde{\mathbf{p}}_0^l\|_1}_{\text{aggregation error}} + \underbrace{\sum_{l=1}^L \sum_{k=1}^{k_l} \sum_{\rho \in \Phi} \boldsymbol{\pi}_{k-1}^l(\rho) \cdot \epsilon^l(\rho)}_{\text{propagation error}} \quad (8)$$

Remark. As was previously mentioned, we do not require on an abstract matrix Π the normalisation condition $\forall \rho \in \Phi: \sum_{\sigma \in \Phi} \Pi(\rho, \sigma) = 1$ to hold: the corresponding abstraction (Φ, Π) might not be an actual DTMC according to Definition 1, see e.g. Figure 1. As a consequence, elements of the abstract ‘probability vectors’ $\boldsymbol{\pi}_k$ might not sum to one. This, however, should not discourage us from using such abstractions: function Π (respectively, $\boldsymbol{\pi}_k$) simply serves as a high-level representative of function P (respectively, \mathbf{p}_k) on a new state space. Since we are able to estimate $\|\mathbf{e}_k\|_1$, these abstractions provide us with valid approximations of their concrete counterparts, as will be confirmed in the experiments presented in Section 5. As it will be argued later, in some situations it might be helpful or necessary for these abstractions to satisfy the normalisation property: to avoid any confusion, we will reserve the term ‘stochastic’ for matrices and vectors that satisfy the normalisation condition. \square

2.3. State-space truncation of DTMC

State-space truncation [6] is yet another approximation technique that can be applied to any Markov chain. Its transient probability distribution is computed similarly to (1), however before each iteration, states with insignificant transient probability, i.e. those with probability below some specified truncation threshold δ_{tru} , are discarded. The effect of this truncation is twofold. First of all, we are now able to propagate probability mass only from *significant* (also called *active*) states, which leads to a speedup of the analysis. On the other hand, each truncated state with a non-zero transient probability contributes to the probability loss and the resulting transient probability distribution $\hat{\mathbf{p}}_k$ is actually an under-approximation of the true distribution \mathbf{p}_k : the probability mass that was truncated could have remained in a given state or might have been transported to other ones. The total probability loss serves as an exact

upper bound on the L_1 -norm of the error vector \mathbf{e}_k :

$$\|\mathbf{e}_k\|_1 = \|\mathbf{p}_k - \hat{\mathbf{p}}_k\|_1 = \|\mathbf{p}_t\|_1 - \|\hat{\mathbf{p}}_t\|_1 = 1 - \|\hat{\mathbf{p}}_t\|_1 = 1 - \sum_{s \in S} \hat{\mathbf{p}}_k(s). \quad (9)$$

The truncation threshold δ_{tru} specifies a trade-off between performance and accuracy: large values of δ_{tru} will discard a considerable number of states for the price of reduced precision, and vice versa. Note that this approach can also be useful for chains with an infinite state space, because at each iteration we can deal only with the (finite) set of active states. This technique fails, however, for chains with slow dynamics of the transient probability: inactive states that slowly receive small accruals of the probability mass never become active if the truncation threshold is not small enough, which can yield an enormous error. In general, this does not happen with the state-space aggregation: working with clusters preserves – at least to some extent – information about where the residual transient probability is located. On the other hand, ϵ -terms might result in rather conservative error bounds, when compared to the actual probability lost from the transitions.

2.4. Continuous-time Markov chains

Definition 2. A continuous-time Markov chain (CTMC) is a pair $C = (S, R)$, where

- S is the set of states, and
- $R: S \times S \rightarrow \mathbb{R}_{\geq 0}, \forall s \in S: R(s, s) = 0$, is the transition rate matrix.

Similar to DTMCs, we will implicitly assume that the set S is finite. R is a function that for each pair of different states assigns a rate used as a parameter of an exponential distribution when deriving a probability of transitioning between these states within a continuous time window. The time spent in state r , before any such transition occurs, is exponentially distributed with parameter $E(r) := \sum_{s \in S} R(r, s)$, which is called the exit rate of state r . An infinitesimal generator matrix associated with C is a matrix $Q: S \times S \rightarrow \mathbb{R}$ defined as $Q(s, s) = -E(s)$ and $Q(r, s) = R(r, s)$ for $r \neq s$.

Definition 3. Let $C = (S, R)$ be a CTMC and Q be its infinitesimal generator matrix. Let $q \geq \max_{s \in S} E(s)$ be a uniformisation rate. A uniformised DTMC of C given uniformisation rate q is a DTMC (S, unif_Q^q) having its transition probability matrix unif_Q^q defined as

$$\text{unif}_Q^q(r, s) = \begin{cases} 1 + \frac{Q(r, s)}{q}, & \text{if } r = s \\ \frac{Q(r, s)}{q}, & \text{otherwise.} \end{cases}$$

A uniformised DTMC serves as a time-discretisation of a CTMC with respect to the fastest event that can occur with rate q . Usually, we select q to be the maximum exit rate from states in S , which corresponds to the shortest mean

residence time of the model, although any value larger or equal to this rate is also usable.

A CTMC is initialised via the probability distribution $\mathbf{p}_0: S \rightarrow [0, 1]$. The transient probability distribution \mathbf{p}_t at an arbitrary time horizon $t \in \mathbb{R}_{\geq 0}$ can be obtained by employing a uniformisation technique. The main idea of this method is to split a CTMC $C = (S, R)$ into two independent stochastic processes D_C and B_C : D_C is a DTMC over the same state space S ; B_C is a CTMC (called a *birth process of C*) having an infinite state space \mathbb{N}_0 , such that

$$\mathbf{p}_t(s) = \sum_{k=0}^{\infty} \mathbf{u}_k(s) \cdot \beta_t(k), \quad (10)$$

where \mathbf{u}_k denotes the transient probability distribution of D_C at time k and $\beta_t(\cdot)$ denotes the transient probability distribution of B_C at time t . Intuitively, Equation (10) invokes the total probability theorem on the number of discrete ‘jumps’ of C taking place up to time t : the quantity $\mathbf{u}_k(s)$ represents the probability of residing in state s after exactly k discrete jumps, whereas $\beta_t(k)$ expresses the probability of actually performing these k jumps within a continuous window of length t . Under this interpretation, D_C keeps track of the current state of C and B_C keeps track – in a probabilistic sense – of whether time t has elapsed.

2.5. Standard uniformisation of CTMC

The choice of D_C and B_C is key for the uniformisation procedure. A *standard uniformisation (SU)* works by selecting a uniformisation rate $q \geq \max_{s \in S} E(s)$, and then choosing D_C to be a uniformised DTMC (S, unif_Q^q) with rate q , and B_C to be a pure birth process with constant rate q (i.e. Poisson process with rate q), for which the analytical solution is known to be $\beta_t(k) = e^{-qt} \frac{(qt)^k}{k!} =: \psi_{qt}(k)$, $k \in \mathbb{N}_0$. Finally, for a given precision (i.e. maximum error) ε_{fg} , the iterative scheme of Fox and Glynn [35] can provide parameters k_L, k_R such that

$$1 - \varepsilon_{fg} \leq \sum_{k=k_L}^{k_R} \psi_{qt}(k). \quad (11)$$

We can then truncate the infinite sum in (10) to obtain an under-approximation $\hat{\mathbf{p}}_t$ of the true probability distribution \mathbf{p}_t , as:

$$\hat{\mathbf{p}}_t(s) = \sum_{k=k_L}^{k_R} \mathbf{u}_k(s) \cdot \psi_{qt}(k) \leq \mathbf{p}_t(s). \quad (12)$$

Combining (11) and (12), we arrive at

$$\begin{aligned}
\|\hat{\mathbf{p}}_t\|_1 &= \sum_{s \in S} \hat{\mathbf{p}}_t(s) = \sum_{s \in S} \sum_{k=k_L}^{k_R} \mathbf{u}_k(s) \cdot \psi_{qt}(k) = \sum_{k=k_L}^{k_R} \sum_{s \in S} \mathbf{u}_k(s) \cdot \psi_{qt}(k) \\
&= \sum_{k=k_L}^{k_R} \psi_{qt}(k) \cdot \sum_{s \in S} \mathbf{u}_k(s) = \sum_{k=k_L}^{k_R} \psi_{qt}(k) \geq 1 - \varepsilon_{fg},
\end{aligned}$$

and therefore

$$\|\mathbf{e}_t\|_1 = \|\mathbf{p}_t - \hat{\mathbf{p}}_t\|_1 = \|\mathbf{p}_t\|_1 - \|\hat{\mathbf{p}}_t\|_1 = 1 - \|\hat{\mathbf{p}}_t\|_1 \leq \varepsilon_{fg},$$

325

as desired. In other words, we have a guarantee that the total probability loss resulting from the truncation of the infinite sum in (10) will not exceed ε_{fg} . Note that this proposition holds since the transient probabilities $\mathbf{u}_k(s)$ sum to one. The main drawback of SU is that for large uniformisation rates q the mean of the Poisson distribution $\psi_{qt}(\cdot)$ is large and so is the upper truncation point k_R . This implies that, in order to obtain $\hat{\mathbf{p}}_t$, one must perform plenty of iterations for the uniformised DTMC D_C .

330

2.6. Adaptive uniformisation of CTMC

As an alternative to SU, *adaptive uniformisation (AU)* [29] allows the rates of the birth process to change at each step, according to the following rules:

335

- let $q \geq \max_{s \in S} \{E(s)\}$ be a (global) uniformisation rate for the CTMC C ;
- let q_0, q_1, \dots be an infinite sequence of (local) uniformisation rates satisfying

$$q \geq q_i \geq \max\{E(s) \mid s \in S, u_i(s) > 0\}; \quad (13)$$

- let $B_C = (\mathbb{N}_0, R_{B_C})$ be a CTMC starting at state 0 and R_{B_C} be defined as

$$R_{B_C}(i, j) = \begin{cases} q_i, & \text{if } j = i + 1 \\ 0, & \text{otherwise;} \end{cases}$$

- let $D_C = (S, \text{unif}_Q^{q_i})$ be a time-inhomogeneous DTMC with transition probability matrix at step i to be a uniformisation of R with rate q_i , and where \mathbf{u}_i denotes its transient probability distribution at time step i .

340

The analysis of a CTMC C via adaptive uniformisation proceeds as follows. We start at a discrete time 0 with a subset of states in S that have non-zero initial transient probability $\mathbf{u}_0(\cdot)$ – such states are called *significant* or *active*. The largest exit rate among the states within this subset is the (local) uniformisation rate q_0 . We then compute $\text{unif}_Q^{q_0}$ to be the transition probability matrix for the process D_C at (discrete) time 0, perform probability propagation and obtain $\mathbf{u}_1(\cdot)$. We then repeat the procedure of defining the subset of active states,

345

finding a (local) uniformisation rate, uniformizing the rate matrix according to this rate and propagating the probability. This way we obtain a sequence $\mathbf{u}_0, \mathbf{u}_1, \dots$, that will be used to compute \mathbf{p}_t according to (10), where $\beta_t(\cdot)$ is a solution to the birth process B_C with rates q_0, q_1, \dots . In order to solve this CTMC, we apply SU using a (global) uniformisation rate q , since $\forall i \in \mathbb{N}_0, q_i \leq q$. Together with the Fox-Glynn method for a given precision ε_{fg} , we can compute an under-approximation $\hat{\beta}_t$ of the transient probabilities β_t at time t of the birth process B_C . The resulting under-approximation of the transient probability distribution $\hat{\mathbf{p}}_t$ is then computed as

$$\hat{\mathbf{p}}_t(s) = \sum_{k=0}^{k'_R} \mathbf{u}_k(s) \cdot \hat{\beta}_t(k), \quad (14)$$

where k'_R is a time step for which $\sum_{k=0}^{k'_R} \hat{\beta}_t(k) \geq 1 - \varepsilon_{bp}$ for a given precision $\varepsilon_{bp} < \varepsilon_{fg}$. Both sum truncations – for uniformising C and uniformising the inner birth process B_C – lead to an under-approximation $\hat{\mathbf{p}}_t$ of the true probability distribution \mathbf{p}_t , and the total error is given by the probability loss $1 - \|\hat{\mathbf{p}}_t\|_1$ with a bound ε_{bp} specified a-priori.

The main advantage of AU is that uniformisation rates q_i are ‘discovered’ as the probability propagates. As there is a chance that at any given time i , q_i will be substantially lower than q , this allows the birth process to jump at lower rates, and therefore that k'_R is substantially lower than the corresponding upper Fox-Glynn limit k_R in the case of SU. Numerically, this allows to perform much fewer vector-matrix multiplications to solve for D_C and to obtain the same result with the same precision as SU. One might argue that the varying uniformisation rate q_i complicates the computation of the transient probabilities \mathbf{u}_k of the uniformised DTMC D_C or the solution $\hat{\beta}_t(k)$ of the birth process B_C : this is true only to a some degree. The birth process B_C still has an extremely simple structure and thus computing $\hat{\beta}_t(k)$ is almost trivial during each iteration. Similarly, a rather simple form of the uniformised transition matrix $\text{unif}_Q^{q_i}$ (see Definition 3) allows to avoid constructing the uniformised DTMC and to perform vector-matrix multiplications directly with the use of the infinitesimal generator Q .

2.7. Beyond uniformisations of CTMC: combined approximations

State-space truncation (not to be confused with the sum truncation in (12) or (14)) can be used with both SU or AU to solve for D_C , although it is particularly favorable with AU since truncating the state space using threshold $\delta_{\text{tru}} > 0$ leads to smaller subsets of active states and the birth process B_C can jump at even slower rates q_i . In the sequel, we will refer to the combination of SU with state-space truncation as *fast SU (FSU)*, and to the combination of AU with truncation as *fast AU (FAU)* [6]. In both of these cases, however, the probability loss is the only way to compute the approximation error, since an a-priori specified error bound cannot be guaranteed.

Finally, SU can be integrated with the state-space aggregation approach while solving for uniformised DTMC. This idea was first outlined in [10], although a rigorous formalisation is still missing and will be the focus of Section 4. There we shall also explore combinations of aggregation and truncation approaches (*FAU+* hybrid scheme).
390

3. State-Space Aggregation of DTMCs

In this section, we develop ideas presented in [10] and formalise a notion of a general state-space aggregation for discrete-time Markov chains. This will allow to explore various aggregation schemes as well as to obtain more precise bounds on the approximation errors. Finally, we describe an aggregation procedure that is capable of handling arbitrary DTMCs. In Section 4 we will then apply these ideas to enable the analysis of continuous-time models.
395

3.1. Approximate DTMCs

We wish to explore how altering the transition probability matrix of a DTMC affects its transient behaviour. We will do so by introducing the concept of an approximate DTMC.
400

Definition 4. Let $D = (S, P)$ be a DTMC. Let $\tilde{P}: S \times S \rightarrow \mathbb{R}$ be an approximation of P with the same dimensions. A pair (S, \tilde{P}) is referred to as an approximation of the DTMC D .

Assume \mathbf{p}_0 and $\tilde{\mathbf{p}}_0$ are initial transient probability distributions of (S, P) and (S, \tilde{P}) , respectively. Here we interpret $\tilde{\mathbf{p}}_0$ as an approximation of \mathbf{p}_0 . We can now compute the transient probability distribution $\tilde{\mathbf{p}}_k$ of the approximate DTMC (S, \tilde{P}) at any time $k > 0$ similarly to propagation Equation (1):
405

$$\tilde{\mathbf{p}}_k = \tilde{\mathbf{p}}_{k-1} \cdot \tilde{P}. \quad (15)$$

The transient probability distribution $\tilde{\mathbf{p}}_k$, $k \geq 0$, serves as an approximation of the distribution \mathbf{p}_k . We are interested in computing an approximation error $\mathbf{e}_k := \tilde{\mathbf{p}}_k - \mathbf{p}_k$. First, observe that \mathbf{e}_0 captures the error associated with approximating \mathbf{p}_0 by $\tilde{\mathbf{p}}_0$. For $k > 0$, it holds that
410

$$\begin{aligned} \mathbf{p}_k + \mathbf{e}_k &= \tilde{\mathbf{p}}_k = \tilde{\mathbf{p}}_{k-1} \cdot \tilde{P} = \tilde{\mathbf{p}}_{k-1} \cdot (\tilde{P} - P + P) = \tilde{\mathbf{p}}_{k-1} \cdot P + \tilde{\mathbf{p}}_{k-1} \cdot (\tilde{P} - P) \\ &= (\mathbf{p}_{k-1} + \mathbf{e}_{k-1}) \cdot P + \tilde{\mathbf{p}}_{k-1} \cdot (\tilde{P} - P) \\ &= \mathbf{p}_{k-1} \cdot P + \mathbf{e}_{k-1} \cdot P + \tilde{\mathbf{p}}_{k-1} \cdot (\tilde{P} - P) \\ &= \mathbf{p}_k + \mathbf{e}_{k-1} \cdot P + \tilde{\mathbf{p}}_{k-1} \cdot (\tilde{P} - P), \end{aligned}$$

which implies
415

$$\mathbf{e}_k = \mathbf{e}_{k-1} \cdot P + \tilde{\mathbf{p}}_{k-1} \cdot (\tilde{P} - P).$$

This recursion provides insight into how an error is generated when we approximate a DTMC. The first summand represents propagation of an existing error as if we were using exact transitions P for probability propagation. On the other hand, the term $\tilde{\mathbf{p}}_{k-1} \cdot (\tilde{P} - P)$ captures an error that is generated at each step between each pair of states while using the approximation $\tilde{\mathbf{p}}_{k-1}$ for \mathbf{p}_{k-1} and \tilde{P} for P . Recall that we are interested in the L_1 -norm of the error vector \mathbf{e}_k , namely:

$$\begin{aligned} \|\mathbf{e}_k\|_1 &= \left\| \mathbf{e}_{k-1} \cdot P + \tilde{\mathbf{p}}_{k-1} \cdot (\tilde{P} - P) \right\|_1 \\ &\leq \|\mathbf{e}_{k-1} \cdot P\|_1 + \left\| \tilde{\mathbf{p}}_{k-1} \cdot (\tilde{P} - P) \right\|_1. \end{aligned}$$

One can easily argue that $\|v \cdot A\|_1 \leq \|v\|_1$ for any vector v and any stochastic matrix A , and therefore expression above becomes

$$\|\mathbf{e}_k\|_1 \leq \|\mathbf{e}_{k-1}\|_1 + \left\| \tilde{\mathbf{p}}_{k-1} \cdot (\tilde{P} - P) \right\|_1. \quad (16)$$

3.2. State-space aggregation of DTMCs

Let us now introduce a specific class of approximate DTMCs: we will reinterpret the above derivation accordingly.

Definition 5. Let $D = (S, P)$ be a DTMC with initial probability distribution \mathbf{p}_0 and let Φ be a clustering of S . Recall that for a cluster $\sigma \in \Phi$, $[\![\sigma]\!]$ denotes the cardinality of set σ , i.e. number of concrete states that comprise this cluster. Let $\Pi: \Phi \times \Phi \rightarrow \mathbb{R}$ be any real-valued matrix relating pairs of clusters and let $\boldsymbol{\pi}_0: \Phi \rightarrow \mathbb{R}$ be a row vector s.t. $\boldsymbol{\pi}_0(\sigma) := \sum_{s \in \sigma} \mathbf{p}_0(s)$. An approximation (S, \tilde{P}) of the DTMC D , where $\tilde{P}(r, s) = \Pi(\rho, \sigma) / [\![\sigma]\!]$, $r \in \rho, s \in \sigma$, with initial distribution $\tilde{\mathbf{p}}_0(s) = \boldsymbol{\pi}_0(\sigma) / [\![\sigma]\!]$, $s \in \sigma$, will be referred to as a *state-space aggregation of D* given an *abstract state space* Φ and an *abstract transition probability function* Π .

Notice that for each two states $s, s' \in \sigma$, it holds that $\tilde{\mathbf{p}}_0(s) = \frac{\boldsymbol{\pi}_0(\sigma)}{[\![\sigma]\!]} = \tilde{\mathbf{p}}_0(s')$. Similarly, for $(r, r' \in \rho)$ and $(s, s' \in \sigma)$ we have that $\tilde{P}(r, s) = \frac{\Pi(\rho, \sigma)}{[\![\sigma]\!]} = \tilde{P}(r', s')$, i.e. matrix \tilde{P} is lumpable [12], and therefore the update Equation (15) yields, for all $s, s' \in \sigma$,

$$\tilde{\mathbf{p}}_k(s) = \sum_{r \in S} \tilde{\mathbf{p}}_{k-1}(r) \cdot \tilde{P}(r, s) = \sum_{r \in S} \tilde{\mathbf{p}}_{k-1}(r) \cdot \tilde{P}(r, s') = \tilde{\mathbf{p}}_k(s').$$

The three equalities above illustrate an important property of the aggregation: any two states from two given clusters have the same approximate transition probability $\tilde{P}(\cdot, \cdot)$ and any two states in a given cluster at any time step $k \geq 0$ share the same approximate transient probability $\tilde{\mathbf{p}}_k(\cdot)$. Introduce the quantity $\boldsymbol{\pi}_k(\sigma) := \sum_{s \in \sigma} \tilde{\mathbf{p}}_k(s)$, $\sigma \in \Phi$, $k > 0$. From the argument above it follows that $\tilde{\mathbf{p}}_k(s) = \boldsymbol{\pi}_k(\sigma) / \llbracket \sigma \rrbracket$ for any $s \in \sigma$. Intuitively, the quantity $\boldsymbol{\pi}_k(\sigma)$ describes probability of residing in one of the states in cluster σ at time step k , whereas $\Pi(\rho, \sigma)$ captures the probability of transitioning into one of the states in cluster σ given that the chain resides in one of the states in cluster ρ .

Finally, for $k > 0$, it holds that:

$$\begin{aligned} \boldsymbol{\pi}_k(\sigma) &= \sum_{s \in \sigma} \tilde{\mathbf{p}}_k(s) = \sum_{s \in \sigma} \sum_{r \in S} \tilde{\mathbf{p}}_{k-1}(r) \cdot \tilde{P}(r, s) = \sum_{s \in \sigma} \sum_{\rho \in \Phi} \sum_{r \in \rho} \tilde{\mathbf{p}}_{k-1}(r) \cdot \tilde{P}(r, s) \\ &= \sum_{s \in \sigma} \sum_{\rho \in \Phi} \sum_{r \in \rho} \frac{\boldsymbol{\pi}_{k-1}(\rho)}{\llbracket \rho \rrbracket} \cdot \frac{\Pi(\rho, \sigma)}{\llbracket \sigma \rrbracket} = \sum_{\rho \in \Phi} \sum_{s \in \sigma} \sum_{r \in \rho} \frac{\boldsymbol{\pi}_{k-1}(\rho)}{\llbracket \rho \rrbracket} \cdot \frac{\Pi(\rho, \sigma)}{\llbracket \sigma \rrbracket} \\ &= \sum_{\rho \in \Phi} \boldsymbol{\pi}_{k-1}(\rho) \cdot \Pi(\rho, \sigma) \cdot \frac{1}{\llbracket \rho \rrbracket \cdot \llbracket \sigma \rrbracket} \sum_{s \in \sigma} \sum_{r \in \rho} 1 = \sum_{\rho \in \Phi} \boldsymbol{\pi}_{k-1}(\rho) \cdot \Pi(\rho, \sigma), \end{aligned}$$

or in matrix notation:

$$\boldsymbol{\pi}_k = \boldsymbol{\pi}_{k-1} \cdot \Pi,$$

which corresponds to Equation (3). Hence, instead of computing approximate transient probabilities for each of the states, we can first aggregate the initial probability distribution \mathbf{p}_0 into $\boldsymbol{\pi}_0$ according to the definition of the latter, compute $\boldsymbol{\pi}_k$ using (3) and then find $\tilde{\mathbf{p}}_k(s)$ as $\boldsymbol{\pi}_k(\sigma) / \llbracket \sigma \rrbracket$ for any state s . A pair (Φ, Π) might be interpreted as a DTMC (where the transition matrix Π is not necessarily stochastic) representing the aggregation of (S, P) and providing the approximation of its probability distribution. As to an error associated with this approximation, we use properties of aggregation to rewrite (16) into (18): the second term in (16) reads:

$$\left\| \tilde{\mathbf{p}}_{k-1} \cdot (\tilde{P} - P) \right\|_1 = \sum_{s \in S} \left| \sum_{r \in S} \tilde{\mathbf{p}}_{k-1}(r) \cdot (\tilde{P}(r, s) - P(r, s)) \right|.$$

Running both summations over clusters and then applying the observation above concerning states within the same cluster yields

$$\begin{aligned}
& \sum_{\sigma \in \Phi} \sum_{s \in \sigma} \left| \sum_{\rho \in \Phi} \sum_{r \in \rho} \tilde{\mathbf{p}}_{k-1}(r) \cdot \left(\tilde{P}(r, s) - P(r, s) \right) \right| \\
&= \sum_{\sigma \in \Phi} \sum_{s \in \sigma} \left| \sum_{\rho \in \Phi} \sum_{r \in \rho} \frac{\boldsymbol{\pi}_{k-1}(\rho)}{\llbracket \rho \rrbracket} \cdot \left(\frac{\Pi(\rho, \sigma)}{\llbracket \sigma \rrbracket} - P(r, s) \right) \right| \\
&= \sum_{\sigma \in \Phi} \sum_{s \in \sigma} \left| \sum_{\rho \in \Phi} \boldsymbol{\pi}_{k-1}(\rho) \sum_{r \in \rho} \left(\frac{\Pi(\rho, \sigma)}{\llbracket \rho \rrbracket \cdot \llbracket \sigma \rrbracket} - \frac{1}{\llbracket \rho \rrbracket} P(r, s) \right) \right| \\
&= \sum_{\sigma \in \Phi} \sum_{s \in \sigma} \left| \sum_{\rho \in \Phi} \boldsymbol{\pi}_{k-1}(\rho) \left(\frac{\Pi(\rho, \sigma)}{\llbracket \sigma \rrbracket} - \frac{1}{\llbracket \rho \rrbracket} \sum_{r \in \rho} P(r, s) \right) \right|.
\end{aligned}$$

470 The following are algebraic manipulations with summations and absolute values:

$$\begin{aligned}
& \sum_{\sigma \in \Phi} \sum_{s \in \sigma} \left| \sum_{\rho \in \Phi} \boldsymbol{\pi}_{k-1}(\rho) \left(\frac{\Pi(\rho, \sigma)}{\llbracket \sigma \rrbracket} - \frac{1}{\llbracket \rho \rrbracket} \sum_{r \in \rho} P(r, s) \right) \right| \\
&\leq \sum_{\sigma \in \Phi} \sum_{s \in \sigma} \sum_{\rho \in \Phi} \boldsymbol{\pi}_{k-1}(\rho) \left| \frac{\Pi(\rho, \sigma)}{\llbracket \sigma \rrbracket} - \frac{1}{\llbracket \rho \rrbracket} \sum_{r \in \rho} P(r, s) \right| \\
&= \sum_{\rho \in \Phi} \sum_{\sigma \in \Phi} \sum_{s \in \sigma} \boldsymbol{\pi}_{k-1}(\rho) \left| \frac{\Pi(\rho, \sigma)}{\llbracket \sigma \rrbracket} - \frac{1}{\llbracket \rho \rrbracket} \sum_{r \in \rho} P(r, s) \right| \\
&= \sum_{\rho \in \Phi} \boldsymbol{\pi}_{k-1}(\rho) \sum_{\sigma \in \Phi} \sum_{s \in \sigma} \left| \frac{\Pi(\rho, \sigma)}{\llbracket \sigma \rrbracket} - \frac{1}{\llbracket \rho \rrbracket} \sum_{r \in \rho} P(r, s) \right|.
\end{aligned}$$

Based on the obtained formulation, let us now define

$$\boldsymbol{\tau}(\rho, \sigma) := \sum_{s \in \sigma} \left| \frac{\Pi(\rho, \sigma)}{\llbracket \sigma \rrbracket} - \frac{1}{\llbracket \rho \rrbracket} \sum_{r \in \rho} P(r, s) \right|, \quad (17)$$

and $\boldsymbol{\tau}(\rho) := \sum_{\sigma \in \Phi} \boldsymbol{\tau}(\rho, \sigma)$. Then for the L_1 -norm of the error vector \mathbf{e}_k it holds that

$$\|\mathbf{e}_k\|_1 \leq \|\mathbf{e}_{k-1}\|_1 + \sum_{\rho \in \Phi} \boldsymbol{\pi}_{k-1}(\rho) \cdot \boldsymbol{\tau}(\rho). \quad (18)$$

475 Note the similarity of the equation above with (6). Furthermore, observe that

$$\begin{aligned}
\tau(\rho, \sigma) &= \sum_{s \in \sigma} \left| \frac{\Pi(\rho, \sigma)}{\llbracket \sigma \rrbracket} - \frac{1}{\llbracket \rho \rrbracket} \sum_{r \in \rho} P(r, s) \right| \leq \llbracket \sigma \rrbracket \cdot \max_{s \in \sigma} \left| \frac{\Pi(\rho, \sigma)}{\llbracket \sigma \rrbracket} - \frac{1}{\llbracket \rho \rrbracket} \sum_{r \in \rho} P(r, s) \right| \\
&= \max_{s \in \sigma} \left| \Pi(\rho, \sigma) - \frac{\llbracket \sigma \rrbracket}{\llbracket \rho \rrbracket} \sum_{r \in \rho} P(r, s) \right| = \epsilon(\rho, \sigma),
\end{aligned}$$

and therefore the τ -terms in (18) provide a better error bound than that in (6) based on ϵ -terms.

3.3. Specific forms of state-space aggregation

480 So far we have assumed nothing about the form of Π : error bound (18) allows arbitrary abstract transition probability matrices. Recall that the matrix Π determines the structure of the approximate transition matrix \tilde{P} . Therefore, we wish to construct Π based on the knowledge of P so that the resulting approximation \tilde{P} is as precise as possible. Let us now be more specific and describe three possible ways to define Π .
485

3.3.1. State-space aggregation based on average incoming transition probabilities

The approximate transition matrix for this aggregation is defined as follows:

$$\Pi_{in}(\rho, \sigma) = \frac{1}{\llbracket \sigma \rrbracket} \sum_{r \in \rho} \sum_{s \in \sigma} P(r, s). \quad (19)$$

490 The intuition behind this equation is that it encompasses the average *incoming* probability to cluster σ from cluster ρ . This shape of the transition matrix Π was previously introduced in [10] and the error bound (6) based on ϵ -terms was derived accordingly.

3.3.2. State-space aggregation based on average outgoing transition probabilities

495 This scheme is similar to the previous one, except that now we utilise average outgoing transition probabilities:

$$\Pi_{out}(\rho, \sigma) = \frac{1}{\llbracket \rho \rrbracket} \sum_{r \in \rho} \sum_{s \in \sigma} P(r, s). \quad (20)$$

Here we demonstrate that outgoing averaging (20) is a natural approach to define transitions between clusters of states. Let $S_k \in S$ be a random variable describing the current state of the DTMC at time $k \geq 0$. Likewise, let $C_k \in \Phi$
500 be a random variable describing in which of the clusters the DTMC resides at time k . Note that, by definition, $P(r, s) = \mathbb{P}(S_{k+1} = s \mid S_k = r)$ and that $\Pi(\rho, \sigma) = \mathbb{P}(C_{k+1} = \sigma \mid C_k = \rho)$. Also, recall that, given that the chain resides in cluster σ , the probability of residing in any of the state $s \in \sigma$ is uniformly distributed between the states. We obtain

$$\begin{aligned}
\Pi(\rho, \sigma) &= \mathbb{P}(C_{k+1} = \sigma \mid C_k = \rho) = \sum_{r \in \rho} \mathbb{P}(C_{k+1} = \sigma, S_k = r \mid C_k = \rho) \\
&= \sum_{r \in \rho} \mathbb{P}(C_{k+1} = \sigma \mid C_k = \rho, S_k = r) \cdot \mathbb{P}(S_k = r \mid C_k = \rho) \\
&= \sum_{r \in \rho} \mathbb{P}(C_{k+1} = \sigma \mid S_k = r) \cdot \frac{1}{\llbracket \rho \rrbracket} = \frac{1}{\llbracket \rho \rrbracket} \cdot \sum_{r \in \rho} \mathbb{P}(C_{k+1} = \sigma \mid S_k = r) \\
&= \frac{1}{\llbracket \rho \rrbracket} \cdot \sum_{r \in \rho} \sum_{s \in \sigma} \mathbb{P}(C_{k+1} = \sigma, S_{k+1} = s \mid S_k = r) \\
&= \frac{1}{\llbracket \rho \rrbracket} \cdot \sum_{r \in \rho} \sum_{s \in \sigma} \mathbb{P}(S_{k+1} = s \mid S_k = r) = \frac{1}{\llbracket \rho \rrbracket} \cdot \sum_{r \in \rho} \sum_{s \in \sigma} P(r, s),
\end{aligned}$$

505

which is $\Pi_{out}(\rho, \sigma)$. As a consequence, the transition probability function Π_{out} has another property, namely that, for each cluster ρ ,

$$\begin{aligned}
\sum_{\sigma \in \Phi} \Pi_{out}(\rho, \sigma) &= \sum_{\sigma \in \Phi} \frac{1}{\llbracket \rho \rrbracket} \sum_{r \in \rho} \sum_{s \in \sigma} P(r, s) = \frac{1}{\llbracket \rho \rrbracket} \sum_{r \in \rho} \sum_{\sigma \in \Phi} \sum_{s \in \sigma} P(r, s) \\
&= \frac{1}{\llbracket \rho \rrbracket} \sum_{r \in \rho} \sum_{s \in S} P(r, s) = \frac{1}{\llbracket \rho \rrbracket} \sum_{r \in \rho} 1 = 1,
\end{aligned}$$

i.e. matrix Π_{out} is *stochastic*, unlike general abstract matrices Π . Since \mathbf{p}_0 is always a stochastic vector, then so is $\boldsymbol{\pi}_0$, by definition. This implies that all vectors $\boldsymbol{\pi}_k$ and therefore all $\tilde{\boldsymbol{p}}_k$ are stochastic as well. So, the abstract chain (Φ, Π_{out}) is actually a DTMC, as per Definition 1. This subtle difference has two benefits. First, from the technical standpoint, this leads to a slightly better approximation compared to the incoming-based scheme (19), as will be shown later. Second, preserving stochasticity of $\tilde{\boldsymbol{p}}_k$ will be the key to integrating aggregation technique with the uniformisation method (see Section 4), in order to enable the aggregating analysis of CTMCs. Finally, observe that, if we use outgoing averaging for the construction of the abstract transition matrix Π , then from (17) it follows that $\boldsymbol{\tau}(\rho, \sigma) = 0$ whenever $\llbracket \sigma \rrbracket = 1$: this is favourable with our partitioning approach (discussed in Subsection 3.4), which utilises singleton clusters for states having large transition probabilities.

520

3.3.3. Median-based state-space aggregation

This scheme is defined as follows:

$$\Pi_{med}(\rho, \sigma) = \frac{\llbracket \sigma \rrbracket}{\llbracket \rho \rrbracket} \operatorname{med}_{s \in \sigma} \left\{ \sum_{r \in \rho} P(r, s) \right\}. \quad (21)$$

The median-based scheme was derived using the following argument. Assume a specific state-space clustering is given. We can arbitrarily define the

525

abstract transition probabilities $\Pi(\cdot, \cdot)$ and the approximation error accrual in each iteration is captured by (18). In order to minimize this accrual, it is sufficient to minimize each of the terms

$$\tau(\rho, \sigma) = \sum_{s \in \sigma} \left| \frac{\Pi(\rho, \sigma)}{\llbracket \sigma \rrbracket} - \frac{1}{\llbracket \rho \rrbracket} \sum_{r \in \rho} P(r, s) \right|$$

530 by selecting a suitable $\Pi(\rho, \sigma)$. We can pull $\llbracket \sigma \rrbracket$ at the denominator out of the absolute value and equivalently minimize

$$\sum_{s \in \sigma} \left| \Pi(\rho, \sigma) - \frac{\llbracket \sigma \rrbracket}{\llbracket \rho \rrbracket} \sum_{r \in \rho} P(r, s) \right|.$$

We recognize this as a problem of minimizing the sum of the absolute deviations, for which solution is known [36] to be

$$\operatorname{med}_{s \in \sigma} \left\{ \frac{\llbracket \sigma \rrbracket}{\llbracket \rho \rrbracket} \sum_{r \in \rho} P(r, s) \right\} = \frac{\llbracket \sigma \rrbracket}{\llbracket \rho \rrbracket} \operatorname{med}_{s \in \sigma} \left\{ \sum_{r \in \rho} P(r, s) \right\} = \Pi_{med}(\rho, \sigma).$$

535

As will be shown in the experimental evaluation, the median-based scheme results in the most accurate error bound. Note that in this case Π_{med} might not be stochastic.

3.4. Partitioning arbitrary DTMCs

540

Before we present our main aggregation algorithm, let us finally address the issue we have ignored so far – how to partition the state space of a DTMC. Recall that previously, in [10], where the state-space aggregation is used to analyse biochemical processes, the partition is constructed based on the known structure of the model and on the underlying physics. Here we wish to establish

545 a procedure capable of handling models with arbitrary structure of their state space. To achieve this, let us view a Markov chain (S, P) as a weighted directed graph (S, E) , where S is the set of its vertices, $E \subseteq S \times S$ is the set of its non-zero transitions and P is the weighting function.

550

Recall during *adaptive* aggregation of a DTMC, we use different clusterings of the state space sequentially in time, based on the current (approximate) probability distribution. These clusterings are constructed based on the so-called *prototype clustering* $\bar{\Phi}$, the computation of which is summarised in Algorithm 1, where Φ^1 denotes the set $\{\{s\} \mid s \in S\}$ of singleton clusters. The procedure employs the nearest-neighbour bottom-up clustering approach, where we start

555 with partition $\bar{\Phi} = \Phi^1$ containing only singletons, which are then sequentially merged so as not to violate the given *maxClusterSize* parameter. For merging, we prioritize clusters ρ and σ containing states r and s having the largest transition weight, that is, the largest transition probability $P(r, s)$, in the spirit of the nearest-neighbour approach.

Algorithm 1 Partitioning the DTMC

Input: DTMC as a directed graph (S, E) with weights P , parameter $maxClusterSize$.

Output: Prototype partition $\bar{\Phi}$.

- 1: $\bar{\Phi} \leftarrow \Phi^1$
 - 2: $E_{sorted} \leftarrow \text{sortDecreasing}(E, P)$
 - 3: **for** $(r, s) \in E_{sorted}$ **do**
 - 4: $\rho \leftarrow \text{clusterOf}(\bar{\Phi}, r)$
 - 5: $\sigma \leftarrow \text{clusterOf}(\bar{\Phi}, s)$
 - 6: **if** $(\rho \neq \sigma) \wedge (\llbracket \sigma \rrbracket + \llbracket \rho \rrbracket \leq maxClusterSize)$ **then**
 - 7: $\bar{\Phi} \leftarrow (\bar{\Phi} \setminus \{\rho, \sigma\}) \cup \{\rho \cup \sigma\}$
 - 8: **return** $\bar{\Phi}$
-

560 Now assume that we wish to aggregate a DTMC at some time k and let $\tilde{\mathbf{p}}_k$ denote the current approximation of transient probabilities. Furthermore, let us introduce the so-called *aggregation threshold* δ_{agg} . Then the resulting clustering Φ is the minimum (in the number of clusters) partition of S for which $\forall \sigma \in \Phi$:

$$(\sigma \in \bar{\Phi} \cup \Phi^1) \wedge \left(\sum_{s \in \sigma} \tilde{\mathbf{p}}_k(s) \leq \delta_{agg} \right).$$

In other words, if a cluster $\sigma \in \bar{\Phi}$ does not violate $\sum_{s \in \sigma} \tilde{\mathbf{p}}_k(s) \leq \delta_{agg}$, then
565 σ is used in the partition Φ , otherwise it is decomposed into singletons.

This rather indirect clustering approach was designed to provide accurate yet efficient approximations of a DTMC. To gauge the accuracy of the clustering, we can use update Equation (18) for the error bound: the product of $\tau(\cdot)$ and $\pi_k(\cdot)$ represents an error contributed by a cluster, and we should minimize $\tau(\cdot)$
570 for clusters that bear a significant probability mass. While experimenting with various partitions, we have often noticed that clusters of large size are typically associated with large values of $\tau(\cdot)$. This makes sense: having (a large amount of) smaller and more refined clusters allows to track the probability mass more accurately than using few large clusters. Figure 2 illustrates the behaviour of
575 both aggregation and propagation errors, with the latter being attributed to a phenomenon we call ‘probability forwarding’: when propagating probability from cluster ρ to cluster σ , we are effectively pushing the probability mass (in one step) to those states in σ that were previously unreachable (in one step) from any of the states in ρ ; conversely, we are pushing the probability to cluster
580 σ from those states in ρ that do not have any of the states in σ as their direct successor. By doing so, we effectively accelerate the model and incur an error.

It should now be clear how the developed clustering approach helps to mitigate this phenomenon. First, during the construction of the prototype clustering, we assemble together states that are actually connected by a (highly
585 likely) transition. As a result, the constructed clusters are comprised of states that are adjacent (likely reachable in a short number of steps), and therefore

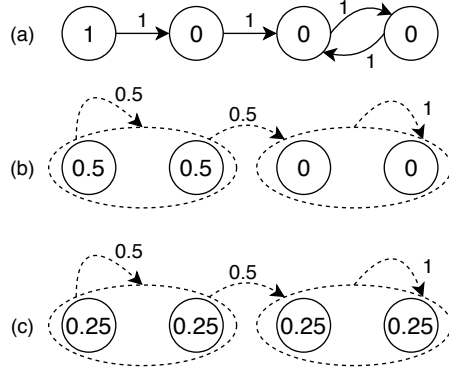


Figure 2: In (a) we consider a simple DTMC that deterministically starts in the leftmost state (numbers inside nodes denote current transient probabilities); in (b) we construct its aggregation (here we use outgoing averaging to compute abstract transitions), notice how the first (second) state has effectively lost (gained) some probability mass, resulting in an aggregation error; in (c) we perform one iteration in the abstract model, observe that the right-most state has effectively gained – due to ‘probability forwarding’ – some probability mass, resulting in a propagation error: in the concrete model this state is unreachable until the third iteration.

the probability forwarding has a lesser effect compared to a situation where the target cluster σ contains states that are otherwise completely unrelated. Second, if the probability $\sum_{s \in \sigma} \tilde{p}_k(s) = \pi_k(\sigma)$ of a (potential) cluster σ exceeds a given aggregation threshold δ_{agg} , then the product $\pi_k(\sigma) \cdot \tau(\sigma)$ would not be insignificant, and, therefore, it is appropriate to split cluster σ into smaller ones – in our case, into singletons.

Finally, using clusters from either the prototype clustering $\bar{\Phi}$ or the singleton partition Φ^1 goes a long way in terms of computational complexity of (re-)aggregation: a great deal of state-to-cluster and cluster-to-cluster data can be pre-computed in advance, allowing for a very efficient construction of the abstract transition probability matrix Π as well as of τ -factors for the given partition Φ , thus enabling more frequent reaggregations of the model, resulting in a more accurate approximation. Naturally, the choice of parameters maxClusterSize and δ_{agg} influences the accuracy as well as efficiency of the provided partitions – these will be discussed shortly, once we establish the adaptive aggregation procedure.

3.5. Adaptive state-space aggregation procedure

Algorithm 2 demonstrates how the theoretical framework developed in the previous subsections is applied to the aggregating analysis of a DTMC. First, we construct the prototype clustering $\bar{\Phi}$, which then used to construct our first *actual* clustering Φ of the state space S (Line 3). Then, we directly apply the corresponding definitions to compute abstract transient probabilities π_0 (see (2)), abstract transition probabilities Π (using either (19), (20) or (21)), error factors τ (see (17)) and the aggregation error $\|e_0\|_1$. We proceed by

Algorithm 2 Adaptive state-space aggregation of DTMC

Input: DTMC (S, P) , initial probability distribution \mathbf{p}_0 , time horizon k ; maximum cluster size $maxClusterSize$, aggregation threshold δ_{agg} , reaggregation threshold δ_{reagg} .

Output: Approximate probability distribution $\tilde{\mathbf{p}}_k$, error bound $\|\mathbf{e}_k\|_1$.

```
1:  $\bar{\Phi} \leftarrow \text{prototypeClustering}(S, P, maxClusterSize)$  ▷ using Alg. 1
2:  $\tilde{\mathbf{p}}_0 \leftarrow \mathbf{p}_0$ 
3:  $\Phi \leftarrow \text{partition}(\bar{\Phi}, \tilde{\mathbf{p}}_0, \delta_{agg})$ 
4:  $(\boldsymbol{\pi}_0, \Pi, \boldsymbol{\tau}, aggregationError) \leftarrow \text{aggregate}(\Phi, P, \tilde{\mathbf{p}}_0)$ 
5:  $error_0 \leftarrow aggregationError$ 
6: for  $i \leftarrow 1$  to  $k$  do
7:    $error_i \leftarrow error_{i-1} + \sum_{\rho \in \Phi} \boldsymbol{\pi}_{i-1}(\rho) \cdot \boldsymbol{\tau}(\rho)$ 
8:    $\boldsymbol{\pi}_i \leftarrow \boldsymbol{\pi}_{i-1} \cdot \Pi$ 
9:   if  $\text{checkPartition}(\Phi, \boldsymbol{\pi}_i, \delta_{reagg})$  then
10:     $\tilde{\mathbf{p}}_i \leftarrow \text{deaggregate}(\boldsymbol{\pi}_i, \Phi)$ 
11:     $\Phi \leftarrow \text{partition}(\bar{\Phi}, \tilde{\mathbf{p}}_i, \delta_{agg})$ 
12:     $(\boldsymbol{\pi}_i, \Pi, \boldsymbol{\tau}, aggregationError) \leftarrow \text{aggregate}(\Phi, P, \tilde{\mathbf{p}}_i)$ 
13:     $error_i \leftarrow error_i + aggregationError$ 
14:  $\tilde{\mathbf{p}}_k \leftarrow \text{deaggregate}(\boldsymbol{\pi}_k, \Phi)$ 
15: return  $\tilde{\mathbf{p}}_k, error_k$ 
```

carrying out vector-matrix multiplications in the abstract setting and updating the error bound according to Equation (18). After several discrete steps, the probability distribution $\boldsymbol{\pi}_i$ might start to generate a large amount of error, which is signalled by the `checkPartition` procedure (Line 9, described later), and the re-partitioning of the state space takes place.

From the computational standpoint, lines 7 and 8 represent the critical parts of Algorithm 2 and are equivalent to computing a scalar product and a vector-matrix multiplication in the abstract setting, i.e. with the reduced state space. In the case where $|\Phi| \ll |S|$, we can achieve a considerable speedup over the computation on the concrete chain, provided that reaggregations are performed not too often (yet not too rarely in order to keep the accrued error relatively low). Intuitively, we want to re-aggregate the chain once the transient probabilities have changed so much that the current clustering might yield a significant error. The `checkPartition` procedure detects this by testing whether the current partition Φ contains a composite cluster with a probability mass exceeding a predefined *reaggregation threshold* δ_{reagg} . After that, a new clustering respecting current probability distribution is established.

The choice of parameters *maxClusterSize*, δ_{agg} and δ_{reagg} offers flexibility and affects the trade-off between efficiency and accuracy. In particular, small values of *maxClusterSize* will lead to a more refined prototype clustering, although the resulting aggregated state space can be large. Large values of aggregation threshold δ_{agg} will preserve a lot of clusters for the actual partition and lead to a greater state-space reduction at a price of decreased precision. Finally,

635 a small value of reaggregation threshold δ_{reagg} usually implies frequent reaggre-
gations and offers greater precision; it is recommended to set this parameter a
couple of orders of magnitude larger than the aggregation threshold δ_{agg} .

4. State-Space Aggregation of CTMCs

Having established an aggregation method for DTMCs, let us now combine
it with a uniformisation technique, in order to analyse continuous-time chains.
640 We begin with SU, where the uniformisation rate is fixed and the application of
aggregation described in the previous section is straightforward: the approach
was already outlined in [10], although a rigorous formalisation is missing and is
offered in this section. We then proceed by combining aggregation with AU, and,
finally, we present a new hybrid method that combines the principles of both
645 state-space aggregation and truncation, and offers an unprecedented flexibility
for analysing continuous-time chains.

4.1. State-space aggregation with standard uniformisation (SU)

Recall that SU works by constructing a uniformised DTMC from the rate
matrix using a single uniformisation rate q ; it proceeds by computing transient
650 probabilities for the DTMC and then weighs them using a Poisson distribution
 $\psi_{qt}(\cdot)$. The Fox-Glynn algorithm provides bounds k_L, k_R that allow to truncate
the infinite sum and compute the overall result, as in (12). The error associated
with this truncation is the probability loss $\|\mathbf{p}_t\|_1 - \|\hat{\mathbf{p}}_t\|_1 = 1 - \|\hat{\mathbf{p}}_t\|_1$ (9).

Now assume we use state-space aggregation to approximate transient proba-
655 bilities \mathbf{u}_k of the uniformised DTMC with the $\tilde{\mathbf{u}}_k$ and obtain an approximation
 $\tilde{\hat{\mathbf{p}}}_t$ of $\hat{\mathbf{p}}_t$ as:

$$\tilde{\hat{\mathbf{p}}}_t(s) := \sum_{k=k_L}^{k_R} \psi_{qt}(k) \cdot \tilde{\mathbf{u}}_k(s). \quad (22)$$

Each $\tilde{\mathbf{u}}_k$ has an associated uncertainty $\|\mathbf{e}_k\|_1$ and each $\tilde{\mathbf{u}}_k$ is weighted with
 $\psi_{qt}(k)$, so the overall error associated with this approximation is

$$\left\| \hat{\mathbf{p}}_t - \tilde{\hat{\mathbf{p}}}_t \right\|_1 = \sum_{k=k_L}^{k_R} \|\mathbf{e}_k\|_1 \cdot \psi_{qt}(k). \quad (23)$$

660 We also lose some probability mass by truncating the infinite summation using
bounds k_L and k_R , and to quantify this loss we use the following lemma.

Lemma 1. Let $\{\mathbf{v}_k\}_{k \in \mathbb{N}_0}$ be an infinite series of vectors and let $\mathbf{v} := \sum_{k=0}^{\infty} w_k \cdot$
 \mathbf{v}_k , where w_k are non-negative scalars for which $\sum_{k=0}^{\infty} w_k = 1$. If norms of \mathbf{v}_k
665 are bounded by some v^* , i.e. $\exists v^* \forall k \in \mathbb{N}_0: \|\mathbf{v}_k\|_1 \leq v^*$, then $\|\mathbf{v}\|_1 \leq v^*$.

Proof.

$$\|\mathbf{v}\|_1 = \left\| \sum_{k=0}^{\infty} w_k \cdot \mathbf{u}_k \right\|_1 \leq \sum_{k=0}^{\infty} w_k \cdot \|\mathbf{u}_k\|_1 \leq \sum_{k=0}^{\infty} w_k \cdot v^* = v^* \sum_{k=0}^{\infty} w_k = v^*.$$

□

Corollary 1. Let $\hat{\mathbf{v}} := \sum_{k=k_L}^{k_R} w_k \cdot \mathbf{v}_k$ be a truncation of v for arbitrary bounds k_L, k_R , where $\{w_k\}$ and $\{\mathbf{v}_k\}$ are consistent with Lemma 1. Then,

$$\|\mathbf{v}\|_1 - \|\hat{\mathbf{v}}\|_1 \leq v^* - \|\hat{\mathbf{v}}\|_1. \quad (24)$$

This corollary asserts that for bounded vectors \mathbf{u}_k used in (12) (or for bounded approximations $\tilde{\mathbf{u}}_k$ of \mathbf{u}_k used in (22)), we are able to compute the probability loss resulting from the truncation of the infinite sum. For SU, AU, FSU or FAU, each of the $\|\mathbf{u}_k\|_1$ is bounded by 1 and so probability loss in (24) takes the usual form $1 - \|\tilde{\mathbf{p}}_t\|_1$. However, for general state-space aggregations, there is no guarantee on the approximations $\tilde{\mathbf{u}}_k$, because we do not require the transition matrices Π to be stochastic. Therefore, in order to safely use aggregation techniques in combination with the Fox-Glynn scheme, it is crucial to appeal to those abstractions for which $\{\tilde{\mathbf{u}}_k\}$ is consistent with Lemma 1. An ideal candidate is the outgoing averaging approach (20) that preserves the stochasticity of vectors $\tilde{\mathbf{u}}_k$, i.e. $\|\tilde{\mathbf{u}}_k\|_1 = 1$, and so the probability loss can be computed analogously to SU/AU. As will be demonstrated on various case studies, outgoing averaging is the most efficient aggregating scheme for the analysis of discrete-time chains.

The rest of the algorithm remains conceptually the same: we work with the abstraction of the uniformised DTMC, where the notions of state adjacency, prototype partition, partition checking, etc. are analogous to those developed in the previous subsection. We compute approximate transient probability distributions of this DTMC that are weighted by Poisson probabilities. The overall error is the sum of the probability loss (similar to (9)) and an approximation error for the uniformised DTMC (23), namely:

$$\|\mathbf{e}_t\|_1 \leq 1 - \|\tilde{\mathbf{p}}_t\|_1 + \sum_{k=k_L}^{k_R} \|\mathbf{e}_k\|_1 \cdot \psi_{qt}(k). \quad (25)$$

690

The combination of the state-space aggregation with SU is denoted SU+.

4.2. State-space aggregation with adaptive uniformisation (AU)

As mentioned earlier, introducing adaptivity to the uniformisation procedure can greatly reduce the required number of discrete steps without any penalty in precision. We wish to incorporate this principle to the aggregating method described above. We cannot apply adaptive uniformisation directly since we have developed the aggregation scheme for (uniformised) DTMCs: we would have to

695

continuously recompute its transition probability matrix each time a uniformisation rate q_i changes (which might happen during each iteration), which is impractical. Instead, we wish to define this matrix as a function of this uniformisation rate. In other words, instead of aggregating uniformised DTMCs, we would like to be able to aggregate the CTMC itself: this will allow us to use AU (or FAU) normally, as it was defined in Subsection 2.6, but on a CTMC with a reduced state space. This notion of an abstract CTMC is introduced in the following definition.

Definition 6. Let (S, R) be a CTMC with infinitesimal generator Q and let Φ be the partition of S . An abstract infinitesimal generator $\Theta: \Phi \times \Phi \rightarrow \mathbb{R}$ is the matrix defined as

$$\Theta(\rho, \sigma) = \frac{1}{\llbracket \rho \rrbracket} \sum_{r \in \rho} \sum_{s \in \sigma} Q(r, s).$$

Furthermore, the exit rate of the abstract state σ is defined as the maximum exit rate of states within this cluster: $E(\sigma) := \max_{s \in \sigma} E(s)$. The structure (Φ, Θ) is called an abstract CTMC.

Let (S, R) be a CTMC and Q be the infinitesimal generator associated with R . Assume a specific state-space aggregation Φ of S and a uniformisation rate q are given. To see why Definition 6 can be applied during the aggregating analysis of a CTMC, it is sufficient to show that aggregation of the uniformised CTMC unif_Q^q is exactly uniformisation unif_Θ^q of the aggregated CTMC from Definition 6. To compute the former, we invoke outgoing averaging (20), since we have already argued that it is the only aggregation strategy that can be safely used for approximating CTMCs:

$$\Pi(\rho, \sigma) = \frac{1}{\llbracket \rho \rrbracket} \sum_{r \in \rho} \sum_{s \in \sigma} \text{unif}_Q^q(r, s), \quad (26)$$

In the case where $\rho \neq \sigma$, we have $\forall r \in \rho \forall s \in \sigma: r \neq s$, so that $\text{unif}_Q^q(r, s) = \frac{Q(r, s)}{q}$ and therefore Equation (26) becomes

$$\Pi(\rho, \sigma) = \frac{1}{\llbracket \rho \rrbracket} \sum_{r \in \rho} \sum_{s \in \sigma} \frac{Q(r, s)}{q} = \frac{1}{q} \cdot \frac{1}{\llbracket \rho \rrbracket} \sum_{r \in \rho} \sum_{s \in \sigma} Q(r, s) = \frac{1}{q} \cdot \Theta(\rho, \sigma) = \text{unif}_\Theta^q(\rho, \sigma).$$

On the other hand, if $\rho = \sigma$, we obtain:

$$\begin{aligned}
\Pi(\rho, \rho) &= \frac{1}{\llbracket \rho \rrbracket} \sum_{r \in \rho} \left[1 + \frac{Q(r, r)}{q} + \sum_{s \in \rho, r \neq s} \frac{Q(r, s)}{q} \right] = \frac{1}{\llbracket \rho \rrbracket} \sum_{r \in \rho} \left[1 + \sum_{s \in \rho} \frac{Q(r, s)}{q} \right] \\
&= \frac{1}{\llbracket \rho \rrbracket} \left[\sum_{r \in \rho} 1 + \sum_{r \in \rho} \sum_{s \in \rho} \frac{Q(r, s)}{q} \right] = 1 + \frac{1}{q} \cdot \frac{1}{\llbracket \rho \rrbracket} \sum_{r \in \rho} \sum_{s \in \rho} Q(r, s) \\
&= 1 + \frac{1}{q} \cdot \Theta(\rho, \rho) = \text{unif}_{\Theta}^q(\rho, \rho).
\end{aligned}$$

Overall, we have $\Pi \equiv \text{unif}_{\Theta}^q$, which completes our proof. One can observe the similarity between Definition 6 of abstract infinitesimal generator and Equation (20) defining the abstract transition probability matrix based on outgoing probability averaging. To recapitulate, we can now avoid computing aggregation \tilde{P} of the uniformised CTMC as a uniformisation of the aggregated CTMC, which does not need to be computed explicitly to propagate probability, as was elaborated in Subsection 2.6. However, we still have to be able to compute bound on the approximation error with similar efficiency. The following proposition demonstrates that it is indeed possible.

Proposition 1. For the error factors $\tau(\cdot)$ associated with partition Φ and abstract transition function Π (based on average outgoing probabilities) of the aggregated uniformised CTMC, the following holds (notice how this expression mirrors Equation (17) derived for the error factors in the discrete-time case):

$$\tau(\rho, \sigma) = \frac{1}{q} \sum_{s \in \sigma} \left| \frac{\Theta(\rho, \sigma)}{\llbracket \sigma \rrbracket} - \frac{1}{\llbracket \rho \rrbracket} \sum_{r \in \rho} Q(r, s) \right|.$$

Proof. Consider the case $\rho \neq \sigma$. Starting from Equation (17), we have:

$$\begin{aligned}
\tau(\rho, \sigma) &= \sum_{s \in \sigma} \left| \frac{\Pi(\rho, \sigma)}{\llbracket \sigma \rrbracket} - \frac{1}{\llbracket \rho \rrbracket} \sum_{r \in \rho} \text{unif}_Q^q(r, s) \right| \\
&= \sum_{s \in \sigma} \left| \frac{1}{\llbracket \sigma \rrbracket} \frac{\Theta(\rho, \sigma)}{q} - \frac{1}{\llbracket \rho \rrbracket} \sum_{r \in \rho} \frac{Q(r, s)}{q} \right| = \frac{1}{q} \sum_{s \in \sigma} \left| \frac{\Theta(\rho, \sigma)}{\llbracket \sigma \rrbracket} - \frac{1}{\llbracket \rho \rrbracket} \sum_{r \in \rho} Q(r, s) \right|.
\end{aligned}$$

If instead $\rho = \sigma$, we have:

$$\begin{aligned}
\tau(\rho, \sigma) &= \sum_{s \in \sigma} \left| \frac{\Pi(\rho, \sigma)}{\llbracket \sigma \rrbracket} - \frac{1}{\llbracket \rho \rrbracket} \sum_{r \in \rho} \text{unif}_Q^q(r, s) \right| \\
&= \sum_{s \in \sigma} \left| \frac{1}{\llbracket \sigma \rrbracket} \left[1 + \frac{\Theta(\rho, \sigma)}{q} \right] - \frac{1}{\llbracket \rho \rrbracket} \left[1 + \frac{Q(r, r)}{q} + \sum_{s \in \sigma, r \neq s} \frac{Q(r, s)}{q} \right] \right| \\
&= \sum_{s \in \sigma} \left| \frac{1}{\llbracket \sigma \rrbracket} + \frac{1}{\llbracket \sigma \rrbracket} \frac{\Theta(\rho, \sigma)}{q} - \frac{1}{\llbracket \rho \rrbracket} - \frac{1}{\llbracket \rho \rrbracket} \sum_{r \in \rho} \frac{Q(r, s)}{q} \right| \\
&= \frac{1}{q} \sum_{s \in \sigma} \left| \frac{\Theta(\rho, \sigma)}{\llbracket \sigma \rrbracket} - \frac{1}{\llbracket \rho \rrbracket} \sum_{r \in \rho} Q(r, s) \right|.
\end{aligned}$$

□

Let us now summarise the aggregating procedure for adaptive uniformisation. We begin by constructing a prototype partition $\bar{\Phi}$ in the same manner as for DTMCs, using Algorithm 1 but using transition rate matrix R as transition weights. Next, we construct an actual partition Φ based on current probability distribution p_0 . Using this partition Φ , we can now compute (1) the corresponding abstract infinitesimal generator Θ , (2) abstract transition probabilities π_0 and (3) for each cluster $\rho \in \Phi$ the value of

$$\sum_{\sigma \in \Phi} \sum_{s \in \sigma} \left| \frac{\Theta(\rho, \sigma)}{\llbracket \sigma \rrbracket} - \frac{1}{\llbracket \rho \rrbracket} \sum_{r \in \rho} Q(r, s) \right|,$$

which, according to Proposition 1, when divided by the current (local) uniformisation rate q_i , will yield the value of $\tau(\rho)$. We now treat (Φ, Θ) as a normal CTMC, albeit with special exit rates, according to Definition 6:

$$q_i \geq \max_{s \in S} \{E(s) \mid \tilde{\mathbf{u}}_i(s) > 0\} = \max_{\sigma \in \Phi} \{E(\sigma) \mid \pi_i(\sigma) > 0\},$$

and pass this aggregated CTMC as an input to the adaptive uniformisation procedure. AU unfolds the model while the partition checker ensures the correctness of the given partition and triggers reclusterings when necessary, using the same heuristics as for DTMCs. The final transition probability as well as the approximation error are computed similarly to (22) and (25) in the case of SU, but using the solution of the birth process as a weighting factor. The described technique, integration of state-space aggregation and adaptive uniformisation, will be denoted as AU+.

4.3. Combination of state-space aggregation with truncation

Finally, we can combine the method above with the state-space truncation where in each iteration we truncate insignificant clusters, i.e. those with transient probability smaller than the truncation threshold δ_{tru} , in order to obtain

755 even smaller uniformisation rates. The resulting technique, denoted FAU+,
 incorporates both state-space aggregation and state-space truncation. The ag-
 gregation threshold δ_{agg} that defines how much of the probability mass can
 constitute a cluster, along with the truncation threshold δ_{tru} defining which ab-
 stract states are to be considered insignificant, drive the overall behaviour of
 the method and offer a great flexibility for handling various types of models,
 760 as will be shown later. On a final note, notice that, when setting aggregation
 and truncation thresholds, we can categorise the approximation techniques as
 in Table 1.

| δ_{agg} | δ_{tru} | Resulting method |
|-----------------------|-----------------------|------------------|
| = 0 | = 0 | AU |
| = 0 | > 0 | FAU |
| > 0 | = 0 | AU+ |
| > 0 | > 0 | FAU+ |

Table 1: Categorisation of the approximation techniques.

5. Experimental Evaluation

765 The goal of this section is to present an exhaustive experimental evaluation
 of approximate methods for the analysis of DTMCs and CTMCs. We will
 start in a discrete-time setting, examine the behaviour of various aggregation
 schemes, evaluate the quality of the theoretical bounds, and finally compare the
 best aggregating strategy against a method based on state-space truncation.
 Finally, we will explore how these methods – including the novel hybrid approach
 770 (FAU+) – compare in the continuous-time setting.

5.1. Experimental setup

All methods are implemented in PRISM 4.3 [7], a state-of-the-art proba-
 bilistic model-checker. We employ its explicit engine, which provides the best
 performance for models of moderate size (up to $\approx 10^7$ states) that do not exhibit
 775 regular or symmetric structures [7]. All the experiments are run on a Debian
 server with 8x Intel Core i7-3770K CPUs (4 cores at 3.5 GHz) and 32 GB RAM,
 with all the algorithms being executed sequentially (1 thread).

The benchmark comprises four models² from different application areas: the
 Lotka-Volterra model [30], a prokaryotic gene expression [37] model, the model
 780 of a workstation cluster [38], and the model of a two-component signalling path-
 way [39]. For the sake of generality and fairness, these models have been chosen
 to cover the broad range of possible behaviours that a stochastic process can ex-
 hibit. For instance, the signalling pathway is characterized by its wide spread of

²All these models are originally in continuous time; discrete-time models are obtained by
 uniformisation, using the (global) uniformisation rate $q_{\text{unif}} = 1.02 \cdot \max_{s \in S} E(s)$.

probability distribution, which limits the reduction capabilities of approximate
 785 methods. On the other hand, the workstation cluster model exhibits complex
 dynamics for the transient probability propagation. The Lotka-Volterra model,
 despite being simple and predictable, has fast dynamics. We will discuss how
 these differences impact the behaviour of individual approximate techniques,
 where aggregation-based methods handle such models differently than those
 790 based on state-space truncation.

5.2. Aggregation of DTMCs

5.2.1. Precision of different aggregation strategies

In our first set of experiments, we will inspect the behaviour of individual
 aggregation schemes in various scenarios for a DTMC. We are interested in the
 795 obtained precision (or accuracy), both empirical (actual distance from the exact
 DTMC solution) and theoretical (derived upper bounds on the L_1 -norm of the
 error vector). To eliminate any model bias, we perform experiments on two
 different models with different sizes and exhibiting distinctive behaviours (see
 Tables 2 and 3). We perform three different experiments, having the following
 800 separate goals:

- Experiment 1 (with outcomes $\mathbf{E1}(\mathbf{e})$, $\mathbf{E1}(\mathbf{t})$): The goal of this experi-
 ment is to compare a one-step behaviour of various abstract transition
 functions. We evolve the model for 100 (concrete) steps, then perform the
 first partitioning and compute abstract transition matrices using three
 805 different approaches: based on average incoming (*In*) or outgoing (*Out*)
 transition probabilities and the median-based strategy (*Med*). Then we
 perform a single step in the abstract model. In all cases we use the same
 value of aggregation threshold and therefore each scheme will be work-
 ing with exactly the same state space partition. We report empirical error
 810 ($\mathbf{E1}(\mathbf{e})$) and the theoretical error bound on the propagation error ($\mathbf{E1}(\mathbf{t})$),
 i.e. $\|\mathbf{e}_{101}\|_1 - \|\mathbf{e}_{100}\|_1$ (that is, we do not take aggregation error $\|\mathbf{e}_{100}\|_1$
 into account, as it would be same in all cases since each technique uses
 the same state-space partition). The differences in the obtained values
 arise only from using different abstract transition matrices. For the case
 815 of average incoming probabilities (*In*), we compute the theoretical bound
 using the ϵ -factors (6), as presented in [10], as well as using newly derived
 τ -terms (18), in order to investigate how the novel bound compares to the
 existing one. As will be repeatedly demonstrated in the following experi-
 ments, τ -factors offer an increase in precision of several orders of magni-
 820 tude, confirming our theoretical conclusions from Subsection 3.2. There-
 fore, for outgoing averaging (*Out*) or median-based aggregation (*Med*),
 we only report the theoretical bound computed using τ -terms.
- Experiment 2 ($\mathbf{E2}(\mathbf{e})$, $\mathbf{E2}(\mathbf{t})$): The goal of this experiment is to demon-
 strate the long-term behaviour of different aggregation approaches. It is
 825 the same as $\mathbf{E1}(\mathbf{e})$ and $\mathbf{E1}(\mathbf{t})$, but after the initial aggregation we perform
 100 consecutive steps without reclusterings. The value reported in $\mathbf{E2}(\mathbf{t})$

is $\|e_{200}\|_1 - \|e_{100}\|_1$, i.e. the bound on the propagation error 100 steps after the first aggregation.

- Experiment 3 (**E3(e)**, **E3(t)**): The goal of this experiment is to investigate the behaviour of various approximations under regular re-aggregations. It is the same as **E2(e)** and **E2(t)**, but in the course of 100 steps after the first aggregation we perform 10 additional reclusterings at fixed times (after iteration 105, 115, 125 etc.). Since for each of the schemes the probability distributions during the corresponding times will be approximately the same and, in this particular case, the *aggregation* error accounts for less than 1% of the overall error, in **E3(t)** we report only the bound on the *propagation* error, see Equation (8).

| | <i>In</i> | | <i>Out</i> | <i>Med</i> |
|--------------|-----------------|-----------------|-----------------|-----------------|
| | ϵ | τ | | |
| E1(e) | 2.07e-23 | 2.07e-23 | 2.51e-23 | 1.93e-23 |
| E1(t) | 1.31e-20 | 1.28e-23 | 1.65e-23 | 9.77e-24 |
| E2(e) | 3.58e-4 | 3.58e-4 | 6.40e-4 | 3.59e-4 |
| E2(t) | 1.33e-1 | 3.86e-4 | 8.95e-4 | 3.71e-4 |
| E3(e) | 2.01e-17 | 2.01e-17 | 2.85e-20 | 3.50e-4 |
| E3(t) | 7.17e-14 | 2.81e-17 | 2.04e-19 | 3.50e-4 |

Table 2: Precision of different aggregation schemes. Model: Lotka-Volterra, dimension of the state space: 160k, aggregation threshold: 1e-25.

| | <i>In</i> | | <i>Out</i> | <i>Med</i> |
|--------------|----------------|----------------|----------------|-----------------|
| | ϵ | τ | | |
| E1(e) | 1.26e-9 | 1.26e-9 | 1.29e-9 | 1.24e-9 |
| E1(t) | 4.39e-6 | 1.07e-10 | 1.27e-10 | 8.09e-11 |
| E2(e) | 1.21e-7 | 1.21e-7 | 1.94e-7 | 1.25e-7 |
| E2(t) | 1.06e-2 | 1.52e-7 | 2.80e-7 | 1.40e-7 |
| E3(e) | 1.02e-7 | 1.02e-7 | 1.68e-8 | 1.27e-7 |
| E3(t) | 2.10e-4 | 1.11e-7 | 3.17e-8 | 1.27e-7 |

Table 3: Precision of different aggregation schemes. Model: Prokaryotic Gene Expression, dimension of the state space: 700k, aggregation threshold: 1e-10.

The results for two different models (with different state-space sizes) are shown in Tables 2 and 3. First, from all experiments we confirm that $In(\epsilon) \ll In(\tau)$, i.e. the newly derived error bound (18) that utilises τ -terms provides several orders of magnitude better bounds than that based on ϵ -terms (6). Second, Experiment 1 shows us that median-based aggregation exhibits the best one-step behaviour, followed by that based on incoming probability, and finally by that based on outgoing probability. Third, in Experiment 2 we see a

845 clear decrease in precision over all the methods: the probability distribution has
 changed and in the absence of reclusterings we obtain a significant error. On the
 other hand, in Experiment 3 we see that reclusterings can drastically improve
 the precision of the approaches based on incoming and outgoing averaging, with
 the latter showing an improvement of a couple of orders of magnitude. Finally,
 850 from Experiments 2 and 3 we confirm that median-based aggregation indeed
 provides the most tight theoretical bound $\mathbf{E}(\mathbf{t})$ on the approximation error $\mathbf{E}(\mathbf{e})$,
 although this error is notably larger than that for averaging-based approaches.

Remark. The difference in the obtained values arises from how individual schemes
 handle the problem of probability forwarding into big clusters. Median-based
 855 aggregation is very likely to select the median transition probability between
 clusters to be equal to zero, because a majority of states in a big target cluster
 would be inaccessible in one step. Hence, no probability forwarding occurs at
 all, and the error is generated by the opposite effect: states that are accessible
 in one step will not get any probability at all. In the long run, it seems to
 860 be ineffective because zero abstract transitions decelerate the model and reag-
 gregations cannot improve this. As a result, median-based aggregation leads
 to a very poor approximation and results in a large empirical error, although
 the theoretical bound remains very tight. Indeed, in the evaluation of large
 models (see experiments presented later), this approach has failed to produce
 865 any reasonable results. Therefore, in the remainder of this experimental eval-
 uation, we abandon the median-based strategy. On the other hand, strategies
 based on averaging always propagate at least some probability mass, and the
 incoming version seems to be advantageous because a large size of a successor
 can alleviate abstract transition probability and probability forwarding is less
 870 apparent as compared to outgoing. The latter, however, seems to yield more
 precise results under regular reclusterings.

5.2.2. Speedup of approximate methods

In the next set of experiments we investigate the speedup of individual approx-
 imation methods. The choice of the model is arbitrary, in the sense that,
 875 in principle, none of the methods are more advantageous than others. We select
 a Lotka-Volterra model of 0.5M states, and compute an approximation of its
 transient probability distribution at time 10000. For a given precision, ranging
 from 1e-1 to 1e-5, each method is tasked with computing as fast as possible
 while guaranteeing this precision; the precision of each method is computed us-
 880 ing τ -factors (18) for outgoing (*Out*), using ϵ - and τ -factors for incoming (*In*)
 averaging, and using probability loss for the state-space truncation (*Tru*). To
 ensure a fair comparison, since none of the approximate methods can guarantee
 a given precision a priori, parameters for each of the methods in each of the
 experiments are tuned individually, on a trial and error basis, in order to obtain
 885 the best computation time w.r.t. a given precision. Results of this experiment
 are presented in Table 4 where we report the speedup with respect to a reference
 computation (10000 usual multiplications of matrices of size 0.5M).

From Table 4, it is clear that $Out > In(\tau) > In(\epsilon)$. The second inequality
 is due to the usage of better theoretical bounds, which means that incoming

| Precision | In | | Out | Tru |
|-----------|------------|--------|--------------|--------------|
| | ϵ | τ | | |
| 1e-5 | 2.650 | 3.181 | 4.715 | 4.541 |
| 1e-4 | 2.785 | 3.201 | 4.789 | 4.541 |
| 1e-3 | 2.785 | 3.201 | 5.206 | 4.720 |
| 1e-2 | 2.935 | 4.059 | 5.712 | 4.944 |
| 1e-1 | 3.380 | 4.059 | 6.029 | 5.142 |

Table 4: Speedup (acceleration w.r.t. concrete computation for guaranteeing a given precision) of various approximate techniques. Model: Lotka-Volterra, dimension of the state space: 0.5M states, discrete time horizon: 10000 steps, execution time of concrete computation: ≈ 120 s

890 averaging that utilised τ instead of ϵ can allow for a larger empirical error
 (by clustering more or reclustering less) to guarantee a certain precision. The
 first inequality can be explained by the fact that, as we have seen previously,
 outgoing averaging is more susceptible to reaggregations, and therefore fewer of
 those are required to guarantee a certain precision. We thus confirm the results
 895 from the first set of experiments. Also, we know that outgoing averaging is
 the only strategy that can be safely used for the analysis of CTMCs, so, from
 now on, under adaptive aggregation we will mean the aggregation based on
 outgoing averaging that utilises τ -terms to quantify the theoretical error - we
 have now repeatedly seen that this approach that preserves the properties of
 900 DTMCs indeed exhibits the best behaviour.

What is new here is an illustration of a behaviour of the state space trun-
 cation Tru , which seems to be inferior to outgoing averaging. To eliminate any
 bias, let us further investigate this relationship by repeating the experiment
 with different models of larger size and with different dynamics. As previously,
 905 we investigate the speedup (acceleration w.r.t. the exact computation) for ag-
 gregation based on outgoing averaging (Out) and truncation (Tru), with both
 guaranteeing a given precision. Table 5 presents the results for the workstation
 cluster model, the uniformised prokaryotic gene expression model and the uni-
 formised two-component signalling pathway. Also, in the third case, instead of
 910 transient analysis, both techniques are applied for a model checking problem
 over the Markov chain model.

In all cases the state-space aggregation has performed considerably better
 than truncation, demonstrating a two- to five-fold acceleration. In order to fur-
 ther investigate why this is the case, let us run a similar experiment as the one
 915 presented in Table 2, where we investigate the precision of the methods. We
 select the same Lotka-Volterra model of size 160k and evaluate it using aggre-
 gation (Out) and truncation (Tru). The experiment goes as follows. First, we
 perform 100 exact steps, then we start approximating using the same aggre-
 gation/truncation threshold: with aggregation, states with probability below
 920 this threshold are aggregated; with truncation, such states are truncated. This
 way we perform 1, 100, 300, 500, 700 or 900 discrete steps more (in the case

| Precision | (a) | | (b) | | (c) | |
|-----------|--------------|------------|--------------|------------|--------------|------------|
| | <i>Out</i> | <i>Tru</i> | <i>Out</i> | <i>Tru</i> | <i>Out</i> | <i>Tru</i> |
| 1e-7 | 9.10 | 6.66 | 21.71 | 7.02 | 11.54 | 4.81 |
| 1e-6 | 10.56 | 7.55 | 28.40 | 9.16 | 14.97 | 5.76 |
| 1e-5 | 11.21 | 8.28 | 35.78 | 9.86 | 16.75 | 6.54 |
| 1e-4 | 16.55 | 8.86 | 40.16 | 10.97 | 18.74 | 7.37 |
| 1e-3 | 17.96 | 9.78 | 51.00 | 11.81 | 24.13 | 8.46 |

Table 5: Speedup (acceleration w.r.t. concrete computation for guaranteeing a given precision) comparison. Models: (a) workstation cluster, dimension of the state space: 1M, time horizon: 10804, execution time of concrete computation: ≈ 300 s; (b) uniformised prokaryotic gene expression; dimension of the state space: 1.2M, time horizon: 10000, execution time of concrete computation: ≈ 300 s; (c) uniformised two-component signalling pathway, population bounds [14,46]; property of interest is time-bounded specification with time horizon of 10000 steps; number of states after PCTL driven transformation: 1M, execution time of concrete computation: ≈ 300 s.

of aggregation, we also perform regular reclusterings, again at fixed times after 10 steps) and in each case we report empirical error (e) and theoretical (t) bound for both methods (for state-space truncation both errors are equal to the probability loss). The results are presented in Table 6. Recall that, contrary to experiments from Tables 4 and 5, both aggregation and truncation use the same threshold.

| Steps | <i>Out(e)</i> | <i>Out(t)</i> | <i>Tru</i> |
|-------|---------------|---------------|------------|
| 101 | 1.2e-8 | 1.4e-8 | 1.0e-8 |
| 200 | 2.1e-7 | 2.3e-6 | 5.2e-7 |
| 400 | 2.6e-7 | 7.7e-6 | 2.0e-6 |
| 600 | 3.1e-7 | 1.5e-5 | 4.1e-6 |
| 800 | 3.2e-7 | 2.0e-5 | 6.2e-6 |
| 1000 | 2.1e-7 | 2.4e-5 | 7.9e-6 |

Table 6: Adaptive aggregation versus state space truncation precision comparison. Model: Lotka-Volterra, dimension of the state space: 160k, aggregation/truncation threshold: 1e-25.

One can see that aggregation gives a better empirical error, which confirms the intuition that aggregating the state space and having at least an approximate idea where the residual probability is located is better than truncating the state space. On the other hand, truncation-based method provide an excellent theoretical bound on the error that ultimately beats the approximation bounds based on τ -terms. However, as Tables 4 and 5 suggest, this does not give truncation an advantage: when allowed to tune parameters individually, outgoing averaging is capable of striking a perfect balance between state-space reduction and number of reclusterings, in order to provide a significantly more efficient approximation.

5.3. Approximation of CTMCs

Now we wish to investigate both uniformisation techniques utilising state-space truncation (FSU & FAU) and combinations of SU & FAU with the state-space aggregation (SU+ & FAU+). The comparison of precision for aggregation versus truncation from the discrete-time case (Table 6) automatically translates to SU+ versus FSU, since now we compute the same transient probabilities of the uniformised model and only weigh them with Poisson probabilities afterwards. The precision comparison involving FAU or FAU+ is trickier instead, because of varying uniformisation rates. However, AU differs from SU only in the total number of iterations and not in the overall precision, so the conclusions from Table 6 can also be applied when comparing SU+/FAU+ with FAU.

We evaluate the overall speedup of individual techniques on various case studies, similarly to Tables 4 and 5. In Table 7, for each of the techniques we report the time acceleration (with respect to SU) to guarantee a given precision.

| Model | Precision | FSU | FAU | SU+ | FAU+ |
|-------|-----------|------|-------------|--------------|--------------|
| (a) | 1e-7 | 4.96 | 5.06 | 9.88 | 9.98 |
| | 1e-6 | 5.34 | 5.75 | 11.61 | 12.18 |
| | 1e-5 | 5.20 | 6.08 | 11.61 | 14.94 |
| | 1e-4 | 5.65 | 8.66 | 17.85 | 20.18 |
| | 1e-3 | 5.79 | 8.67 | 21.70 | 29.58 |
| (b) | 1e-7 | 4.95 | 6.17 | 11.28 | 12.54 |
| | 1e-6 | 5.07 | 6.63 | 12.16 | 13.77 |
| | 1e-5 | 5.07 | 7.02 | 12.64 | 15.38 |
| | 1e-4 | 5.22 | 7.31 | 13.72 | 16.52 |
| | 1e-3 | 5.38 | 7.58 | 14.48 | 18.26 |
| (c) | 1e-7 | 3.23 | 5.55 | 4.69 | 5.00 |
| | 1e-6 | 3.66 | 5.95 | 5.54 | 6.13 |
| | 1e-5 | 4.31 | 6.80 | 6.54 | 7.29 |
| | 1e-4 | 5.08 | 7.81 | 7.45 | 8.93 |
| | 1e-3 | 6.07 | 9.08 | 9.12 | 11.86 |

Table 7: Speedup (acceleration w.r.t. SU for guaranteeing a given precision) comparison. Models: (a) workstation cluster, dimension of the state space: 1M, upper Fox & Glynn bound: 10804, execution time of concrete computation: ≈ 300 s; (b) Lotka-Volterra, dimension of the state space: 1M, upper FG bound: 10117, execution time of concrete computation: ≈ 300 s; (c) signalling pathway, dimension of the state space: 1M, upper FG bound: 11013, execution time of concrete computation: ≈ 300 s

First, we observe that FSU is, without a doubt, inferior to both FAU and SU+. This is consistent with our intuition: FAU is capable to perform fewer discrete steps (approximately twice fewer) by varying the uniformisation rate; SU+ is better than FSU due to the same reasons why aggregation is generally favored against truncation for the DTMC analysis. Next, comparing FAU and SU+, we notice that for workstation cluster and Lotka-Volterra models aggregation is

clearly the preferable approach, while for the signalling pathway FAU slightly outperforms aggregation. This example showcases how the model dynamics can influence the behaviour of the approximation method. While investigating the differences between these models, we have observed that in the first two cases – workstation cluster and Lotka-Volterra – a relatively small set of states maintains the majority of the probability mass, as compared to the signalling pathway where the probability distribution is “flatter”. This difference implies that the state space of the first two models can be reduced much more, compared to the signalling pathway case (approximately 50x against 10x) and, as we can see, aggregation can benefit from this reduction much more. This may be attributed to the fact that the aggregation method initially operates on clusters (and there are clearly fewer of those of concrete states), which are then being adaptively deaggregated into singletons during the analysis. FAU, on the other hand, is capable of ‘discovering’ a newly active state (as opposed to newly active clusters) during probability transition, which, intuitively, seems to be more precise. However, for a small set of active states, as in the case of the workstation cluster of a Lotka-Volterra model, working with clusters to make use of the greater state space reduction (and then reaggregate more frequently to compensate for a minor precision loss) gives SU+ a two-fold advantage over FAU.

With regards to the hybrid FAU+ method, we can see that, in general, it manages to achieve balance between aggregation and truncation and, as a result, it noticeably outperforms standalone methods. However, this flexibility comes with a minor (but easily fixable) downside: the algorithm for this method is parametrized by variables (encompassing thresholds) associated with both aggregation and truncation, and it may not be apparent how to combine them to analyse a given method. The experimental evaluation of the method has shown that an optimal solution is to set the aggregation threshold δ_{agg} to be one to two orders of magnitude larger than the truncation threshold δ_{tru} . Indeed, we first aggregate states into clusters based on the first parameter and then truncate those abstract states according to the second one. On the one hand, if the truncation threshold δ_{tru} is considerably smaller than the aggregation threshold δ_{agg} , the resulting method behaves more like AU+ (only clustering). On the other hand, if both thresholds have close values, the resulting method closely resembles FAU (no clustering). In both cases, we give up the granularity of the abstract state space and thus we lose the main benefit of the hybrid approach.

6. Conclusions

The experimental evidence leads to several conclusions. First, we have explored various aggregation schemes and shown that the newly derived theoretical bound that utilises τ -factors provides a significant precision improvement over the existing bounds based on ϵ -terms. As a result, we have obtained an aggregation method that significantly outperforms truncation-based approach in the discrete case. Equipped with this method, we have designed an analogous aggregation technique for CTMCs and shown that it can provide an efficient

approximation, both for transient analysis and for model checking problems. Second, we have investigated approaches based on aggregation and truncation, have observed how the model dynamics impacts the behaviour of the approx-
imate methods, and have managed to distinguish classes of models for which
1005 aggregation-based methods are more appropriate than truncation-based, and
vice-versa. Finally, we have succeeded to integrate both approaches into a new
hybrid method (FAU+): its inherent flexibility handles models of arbitrary dy-
namics and, as a result, outmatches all existing methods.

1010 *Acknowledgment*

This work has been partially supported by the Czech Science Foundation grant GJ20-02328Y (R. Andriushchenko), the Czech Ministry of Education, Youth and Sports project LL1908 of the ERC.CZ programme (M. Češka), the HICLASS project 113213 (through a partnership between ATI, BEIS and Inno-
1015 vate UK), the PITCH-IN project, and the EPSRC-IAA grant (A. Abate).

References

- [1] C. Baier, E. M. Hanh, B. R. Haverkort, H. Hermanns, J.-P. Katoen, Model checking for performability, *Mathematical Structures in Computer Science* 23 (4) (2013) 751–795.
- 1020 [2] G. Bolch, S. Greiner, H. de Meer, K. S. Trivedi, *Queueing Networks and Markov Chains: Modeling and Performance Evaluation with Computer Science Applications*, Wiley-Interscience, New York, NY, USA, 1998.
- [3] C. Madsen, C. J. Myers, N. Roehner, C. Winstead, Z. Zhang, Utilizing stochastic model checking to analyze genetic circuits, in: *Computational Intelligence in Bioinformatics and Computational Biology (CIBCB)*, IEEE, 2012, pp. 379–386.
- 1025 [4] L. Cardelli, M. Kwiatkowska, M. Whitby, Chemical reaction network designs for asynchronous logic circuits, in: *DNA Computing and Molecular Programming*, Springer, 2016, pp. 67–81.
- 1030 [5] J. Hey, R. Nielsen, Integration within the Felsenstein equation for improved Markov chain Monte Carlo methods in population genetics, *Proceedings of the National Academy of Sciences* 104 (8) (2007) 2785–2790.
- [6] F. Didier, T. A. Henzinger, M. Mateescu, V. Wolf, Fast adaptive uniformization of the chemical master equation, in: *High Performance Computational Systems Biology*, 2009, pp. 118–127.
- 1035 [7] M. Kwiatkowska, G. Norman, D. Parker, PRISM 4.0: Verification of probabilistic real-time systems, in: *Computer Aided Verification (CAV)*, Springer, 2011, pp. 585–591.

- 1040 [8] C. Dehnert, S. Junges, J.-P. Katoen, M. Volk, A Storm is coming: A modern probabilistic model checker, in: *Computer Aided Verification (CAV)*, Springer, 2017, pp. 592–600.
- [9] A. Hartmanns, H. Hermanns, The Modest Toolset: An integrated environment for quantitative modelling and verification, in: *Tools and Algorithms for the Construction and Analysis of Systems (TACAS)*, Springer, 2014, pp. 593–598.
- 1045 [10] A. Abate, L. Brim, M. Češka, M. Kwiatkowska, Adaptive aggregation of Markov chains: Quantitative analysis of chemical reaction networks, in: *Computer Aided Verification (CAV)*, Springer, 2015, pp. 195–213.
- [11] J. G. Kemeny, J. L. Snell, et al., *Finite markov chains*, Vol. 356, van Nostrand Princeton, NJ, 1960.
- 1050 [12] P. Buchholz, Exact and ordinary lumpability in finite markov chains, *Journal of Applied Probability* 31.
- [13] P.-J. Courtois, *Decomposability: Queueing and Computer System Applications*, 1977.
- 1055 [14] G. Franceschinis, R. R. Muntz, Bounds for quasi-lumpable markov chains, *Performance Evaluation* 20 (1) (1994) 223 – 243.
- [15] L. Truffet, Near complete decomposability: Bounding the error by a stochastic comparison method, *Advances in Applied Probability* 29 (3) (1997) 830855.
- 1060 [16] N. Pekergin, T. Dayar, D. N. Alparslan, Componentwise bounds for nearly completely decomposable markov chains using stochastic comparison and reordering, *European Journal of Operational Research* 165 (3) (2005) 810 – 825.
- [17] T. Dayar, N. Pekergin, Stochastic comparison, reorderings, and nearly completely decomposable markov chains, in: *Proceedings of the International Conference on the Numerical Solution of Markov Chains (NSMC99)*, (Ed. Plateau, B. Stewart, W.), Prensas universitarias de Zaragoza, 1999, pp. 228–246.
- 1065 [18] K. G. Larsen, A. Skou, Bisimulation through probabilistic testing, *Information and Computation* 94 (1) (1991) 1–28.
- [19] J. Desharnais, F. Laviolette, M. Tracol, Approximate analysis of probabilistic processes: Logic, simulation and games, in: *Quantitative Evaluation of Systems (QEST)*, 2008, pp. 264–273.
- 1070 [20] A. D’Innocenzo, A. Abate, J.-P. Katoen, Robust PCTL model checking, in: *Hybrid Systems: Computation and Control (HSCC)*, ACM, 2012, pp. 275–285.
- 1075

- [21] A. Abate, J.-P. Katoen, J. Lygeros, M. Prandini, Approximate model checking of stochastic hybrid systems, *European Journal of Control* 16 (6) (2010) 624 – 641.
- 1080 [22] S. E. Z. Soudjani, A. Abate, Adaptive and sequential gridding procedures for the abstraction and verification of stochastic processes, *SIAM Journal on Applied Dynamical Systems* 12 (2) (2013) 921–956.
- [23] S. E. Z. Soudjani, A. Abate, Precise approximations of the probability distribution of a Markov process in time: an application to probabilistic invariance, in: *Tools and Algorithms for the Construction and Analysis of Systems (TACAS)*, Springer, 2014, pp. 547–561.
- 1085 [24] V. Chellaboina, S. P. Bhat, W. M. Haddad, D. S. Bernstein, Modeling and analysis of mass-action kinetics, *IEEE Control Systems Magazine* 29 (4) (2009) 60–78.
- 1090 [25] L. Cardelli, M. Tribastone, M. Tschaikowski, A. Vandin, Maximal aggregation of polynomial dynamical systems, *Proceedings of the National Academy of Sciences* 114 (38) (2017) 10029–10034.
- [26] J. Hasenauer, V. Wolf, A. Kazeroonian, F. Theis, Method of conditional moments (MCM) for the chemical master equation, *Journal of Mathematical Biology* 69 (3) (2014) 687–735.
- 1095 [27] L. Cardelli, M. Kwiatkowska, L. Laurenti, A stochastic hybrid approximation for chemical kinetics based on the linear noise approximation, in: *Computational Methods in Systems Biology (CMSB)*, Springer, 2016, pp. 147–167.
- 1100 [28] M. Češka, J. Křetínský, Semi-quantitative abstraction and analysis of chemical reaction networks, in: *Computer Aided Verification (CAV)*, Springer, 2019, pp. 475–496.
- [29] A. P. A. van Moorsel, W. H. Sanders, Adaptive uniformization, *Communications in Statistics. Stochastic Models* 10 (3) (1994) 619–647.
- 1105 [30] D. T. Gillespie, Exact stochastic simulation of coupled chemical reactions, *The journal of Physical Chemistry* 81 (25) (1977) 2340–2361.
- [31] J. Goutsias, Quasiequilibrium approximation of fast reaction kinetics in stochastic biochemical systems, *The Journal of Chemical Physics* 122 (18) (2005) 184102.
- 1110 [32] H. Salis, Y. Kaznessis, Accurate hybrid stochastic simulation of a system of coupled chemical or biochemical reactions, *The Journal of Chemical Physics* 122 (5) (2005) 054103.
- [33] Y. Cao, D. T. Gillespie, L. R. Petzold, The slow-scale stochastic simulation algorithm, *The Journal of Chemical Physics* 122 (1) (2005) 014116.

- 1115 [34] B. Hepp, A. Gupta, M. Khammash, Adaptive hybrid simulations for multi-scale stochastic reaction networks, *The Journal of Chemical Physics* 142 (3) (2015) 034118.
- [35] B. L. Fox, P. W. Glynn, Computing Poisson probabilities, *Communications of the ACM (CACM)* 31 (4) (1988) 440–445.
- 1120 [36] N. C. Schwertman, A. J. Gilks, J. Cameron, A simple noncalculus proof that the median minimizes the sum of the absolute deviations, *The American Statistician* 44 (1) (1990) 38–39.
- [37] A. M. Kierzek, J. Zaim, P. Zielenkiewicz, The effect of transcription and translation initiation frequencies on the stochastic fluctuations in prokaryotic gene expression, *The Journal of Biological Chemistry* 276 (11) (2001) 8165–8172.
- 1125 [38] B. Haverkort, H. Hermanns, J.-P. Katoen, On the use of model checking techniques for dependability evaluation, in: *Reliable Distributed Systems*, IEEE, 2000, pp. 228–237.
- 1130 [39] M. Češka, D. Šafránek, S. Dražan, L. Brim, Robustness analysis of stochastic biochemical systems, *PLOS ONE* 9 (4) (2014) 1–23.